CONTROLS OVER TUNDRA NON-GROWING SEASON CARBON LOSS

By

ELIZABETH E. WEBB

A THESIS PRESENTED TO THE GRADUATE SCHOOL
OF THE UNIVERSITY OF FLORIDA IN PARTIAL FULFILLMENT
OF THE REQUIREMENTS FOR THE DEGREE OF
MASTER OF SCIENCE

UNIVERSITY OF FLORIDA

2014

ACKNOWLEDGMENTS

I thank Peter Ganzlin, John Krapek, Tom Lane, John Wood, and the researchers and technicians of the Bonanza Creek LTER for their assistance with fieldwork and logistics; the members of the UF Ecosystem Dynamics Research Lab for their help vetting ideas and with the writing process; Kiva Oken for statistical support; David Risk for the allowing me to use the Flux Lab flux generator and, along with Nick Nickerson, aid in on-plot chamber flux calculations; Rosvel Bracho for processing the eddy covariance data; the members of my M.S. committee: Sue Natali, and Tim Martin for their support and constructive criticism and my major advisor, Ted Schuur for his guidance and feedback through every step of this endeavor. Funding for this project was provided by the National Science Foundation CAREER program, the Bonanza Creek LTER program, Denali National Park and Preserve Vital Signs Monitoring Program, and the Department of Energy Terrestrial Ecosystem Processes Program.

TABLE OF CONTENTS

page

LIST OF TABLES

LIST OF FIGURES

LIST OF ABBREVIATIONS

C	Carbon
CiPEHR	Carbon in permafrost experimental heating research
CO_2	Carbon dioxide
EC	Eddy covariance
DOS	Day of season
GPP	Gross primary productivity
NEE	Net ecosystem exchange
NGS	Non-growing season
PAR	Photosynthetically active radiation
R_{eco}	Ecosystem respiration

Abstract of Thesis Presented to the Graduate School
of the University of Florida in Partial Fulfillment of the
Requirements for the Degree of Master of Science

CONTROLS OVER TUNDRA NON-GROWING SEASON CARBON LOSS

By

Elizabeth E. Webb

May 2014

Chair: Edward A.G. Schuur
Major: Botany

Permafrost soils store roughly 1672 Pg of carbon (C), twice the amount currently in the earth's atmosphere. But as high latitudes warm, this temperature-protected C reservoir will become vulnerable to higher rates of decomposition. In recent decades, air temperatures in the high latitudes have warmed more than other region globally, particularly during the winter. Over the coming century, the arctic winter is also expected to experience the most warming of any region or season, yet it is notably understudied. Though warming has been shown to increase plant productivity during the growing season, these seasonal C gains may be offset on an annual basis by C losses during the non-growing season (NGS). Here we present NGS CO_2 flux data from the Carbon in Permafrost Experimental Heating Research (CiPEHR) project, a tundra ecosystem warming experiment in interior Alaska. Our goals were to compare methods of measuring winter CO_2 flux, determine the environmental controls of winter CO_2 flux, account for subnivean photosynthesis and late fall plant C uptake in our estimate of NGS CO_2 exchange, and quantify the effect of warming on total NGS CO_2 flux.

CHAPTER 1
INTRODUCTION

Cold and wet conditions in the high latitudes have limited microbial decomposition of soil carbon (C), and as a result these soils have been accumulating C over the past several millennia (Harden *et al.*, 1992; Trumbore & Harden, 1997; Hobbie *et al.*, 2000; Hicks Pries *et al.*, 2011). Permafrost soils hold half of the world's belowground organic C pool and store twice as much C as is currently in the atmosphere (Tarnocai *et al.*, 2009). However, as a result of climate change, temperatures in high latitudes have increased and are projected to rise more than any other region globally (Christensen *et al.*, 2013a). As permafrost thaws, the magnitude and direction of future permafrost soil C storage are uncertain (Shaver *et al.*, 1992; Oechel *et al.*, 1993, 2000; Schuur *et al.*, 2008, 2013; Koven *et al.*, 2011; Sistla *et al.*, 2013).

It is well documented that warming stimulates plant growth as well as ecosystem respiration (R_{eco}) in tundra ecosystems (Rustad *et al.*, 2001; Oberbauer *et al.*, 2007; Ueyama *et al.*, 2013). In some cases, experimental warming has caused R_{eco} to increase more strongly than plant growth during the growing season (Oberbauer *et al.*, 2007; Biasi *et al.*, 2008), thus increasing the release of C to the atmosphere. Other warming experiments and observational studies on the tundra show that increased C uptake by plants during the growing season outweighs the concurrent increase in R_{eco}, causing the tundra to act as a growing season C sink (Huemmrich *et al.*, 2010; Natali *et al.*, 2011; Trucco *et al.*, 2012; Ueyama *et al.*, 2013). Whether these seasonal C gains are offset during the non-growing season (NGS), however, is dependent on the magnitude of winter R_{eco}. It is particularly important that we understand winter C

dynamics because future warming is predicted to be greatest during winter, increasing on average 4.8 °C by 2100 as compared to 2.2 °C during the summer months over the same time period (Christensen *et al.*, 2013a). Nevertheless, there are few field measurements conducted during this season and winter C fluxes remain a key unknown in estimating the annual C balance of the tundra (Jones *et al.*, 1999; Euskirchen *et al.*, 2012; Belshe *et al.*, 2013).

In a review of wintertime CO_2 fluxes from arctic tundra, Björkman et al. (2010) found estimates of cumulative winter C loss ranged from 0.19 to 210 g CO_2-C m^2 yr^{-1}. This wide range is due in part to poorly understood environmental drivers of winter R_{eco}. As such, the gap-filling methods used to extrapolate over months of missing data are poorly developed. Soil temperature (Oechel *et al.*, 1997; Elberling, 2007; Sullivan *et al.*, 2008, Natali et al. in press), vegetation type (Jones *et al.*, 1999; Grogan, 2012), and snow depth (Fahnestock *et al.*, 1998; Nobrega & Grogan, 2007) have all been linked to field measurements of winter CO_2 flux, but studies often lack sufficient data to create gap-filling models. Furthermore, it is largely thought that soil moisture also plays an important role in winter R_{eco} on the tundra (Fahnestock *et al.*, 1998; Vogel *et al.*, 2009; Grogan, 2012), but its effect has only been documented in laboratory settings (Panikov *et al.*, 2006; Tilston *et al.*, 2010).

The broad range of winter C loss estimates is also attributable to the discrepancies in how winter is defined; winter CO_2 flux measurements are interpolated over different time periods depending on the study. Like many others, Fahnestock et al. (1998) define winter by calendar days that generally coincide with the snow-covered season and assume that only respiration occurs during this time. While this is a

convenient and consistent way to partition the year, it does not allow for inter-annual variation in snow cover nor does it take subnivean photosynthesis into account. Grogan and Jonasson (2006) improved the calendar definition by delineating winter as the continuous period during which mean diel soil temperature at 3 cm was less than 0.5°C and Oechel *et al.* (in press) use a metric based on net radiation to define seasonality. However, photosynthesis does occur under the snow pack and while the soil is frozen (Tieszen, 1974; Kappen, 1993; Starr & Oberbauer, 2003) and assuming that only respiration occurs during these times may over-estimate C release if plant uptake is significant.

In addition to the relatively small amount of winter R_{eco} data available, there are a variety of methods used to measure $R_{eco,}$ all with different assumptions. Different methods often produce different estimates of CO_2 flux even at the same site. A popular method is to measure the concentration of CO_2 within the snowpack and calculate a flux based on Fick's first law (Fahnestock *et al.*, 1998; Jones *et al.*, 1999; Sullivan *et al.*, 2008; Björkman *et al.*, 2010a). Due to the heterogeneity of arctic snow packs, however, ensuring that the vertical diffusion of CO_2 is accurately measured without CO_2 diversion to lateral flow or lost during snow pack venting events can be difficult. Soda lime adsorption is also widely employed (Grogan & Chapin, 1999; Welker *et al.*, 2000; Nobrega & Grogan, 2007; Sjögersten *et al.*, 2008; Rogers *et al.*, 2011) and is especially useful in remote locations where other methods are impractical for extended periods of time because of adverse travel and weather conditions. At sites with the requisite power requirements, eddy covariance (EC) towers are also used to gather data with limited presence of field personnel (e.g. Belshe *et al.*, 2012; Euskirchen *et al.*, 2012,

Oechel *et al.* 2014). Because EC towers can gather data continuously, including during conditions that are dangerous to people, the sheer amount of data generated is a powerful tool to answer high-resolution questions about C flux. The EC method, however, cannot measure over small scales and thus cannot be used on small-scale experimental plots such as in this study. Lastly, chamber measurements (e.g. Grogan & Jonasson, 2006; Elberling, 2007; Vogel *et al.*, 2009; Morgner *et al.*, 2010) are a good way to measure temporal variability (and associated environmental controls over R_{eco}) on a small scale, but are labor intensive, can only be performed in favorable weather conditions, and are sensitive to pressure changes that can affect flux estimates. Often chamber measurements are performed by removing snow and placing a chamber directly over the soil but this technique disturbs the local snow pack, affecting snow-mediated soil insulation when sampling is repeated on the same plots. In contrast, chambers that remain under the snow for the duration of the winter are understudied but may affect the CO_2 diffusion gradient between the soil and ambient snow pack. Thus, due to the harshness of the arctic winter environment, evaluations of measurement accuracy and error are limited and there is no standardized method of measuring winter R_{eco}.

Because winter measurements and associated CO_2 flux models form a key component of the annual C balance calculations, accurately understanding the environmental controls of winter R_{eco}, defining winter, and recognizing the biases associated with winter measurement methods are critical steps to ensure accurate analysis. To understand the role of winter processes under likely climate change scenarios, we measured CO_2 flux at the Carbon in Permafrost Experimental Research

(CiPEHR) project, a tundra warming experiment in interior Alaska. Our goals were four-fold: (1) to identify the drivers of winter R_{eco}, (2) to define winter such that photosynthetic activity was accurately incorporated, (3) to compare methods of measuring winter flux, and (4) to quantify the effect of warming on NGS CO_2 loss.

CHAPTER 2
MATERIALS AND METHODS

Site Description

The CiPEHR field site is located in the northern foothills of the Alaska Range near Denali National Park and Preserve (63°52'59' N, 149°13'32' W) in the Eight Mile Lake (EML) watershed, Alaska (Figure 2-1; Schuur *et al.*, 2009; Natali *et al.*, 2011; Trucco *et al.*, 2012). The vegetation at the site is moist acidic tundra at an elevation of 700m on a relatively well-drained gentle northeast-facing slope (Natali *et al.*, 2012). Mean annual air temperature is -2.8°C (2008-2013) and -11.3°C for the October-April period (Table 2-1). The EML watershed is within the zone of discontinuous permafrost, but the entire field site is underlain by permafrost; the average active layer is 57.9 ± 1.9 cm for control plots and 65.8 ± 3.4 cm for warmed plots (standard error, n=5 years: 2009-2013). Permafrost temperatures have been monitored in the EML region since 1985 and document regional permafrost thaw over the past three decades (Osterkamp *et al.*, 2009). Permafrost degradation has also been documented by more extensive measurements of CO_2 fluxes, active layer depth, aboveground biomass, and radiocarbon at a nearby natural permafrost thaw gradient since 2004 (Schuur *et al.*, 2007, 2009; Vogel *et al.*, 2009; Lee *et al.*, 2011; Belshe *et al.*, 2012; Trucco *et al.*, 2012; Hicks Pries *et al.*, 2013).

Experimental Design

Soil warming at CiPEHR is achieved using snow fences (n=6) distributed throughout the landscape in three experimental blocks (Figure 2-1). The fences, which are installed in September of each year and removed in the spring, cause snow to accumulate preferentially on the warming (leeward) side of the fence. This increased

snow pack insulates the soil and the soil in the treated plots is on average 1.5 °C warmer during October-April (Table 2-1), with the bulk of this warming occurring in the late winter (December-April) after snow has accumulated (Natali *et al.*, 2011, 2012, 2014). In the early spring, the increased snow layer is removed to prevent delayed melt out. This soil warming treatment has been ongoing since the winter of 2008-2009 and the sustained warming has resulted in surface permafrost degradation (Natali *et al.* 2014).

Ecosystem C Fluxes

Net ecosystem exchange (NEE) is the net gain or loss of C to an ecosystem over a set amount of time. NEE comprises both R_{eco} and plant C uptake (gross primary productivity; GPP) such that NEE = R_{eco} - GPP. R_{eco} can be measured during dark periods when GPP is assumed to be zero and NEE can be measured at all times; GPP is inferred from the difference between NEE and R_{eco}. We used the convention that negative NEE values denote net C uptake by the ecosystem.

Field Measurements

On-plot Chamber Measurements

In late September 2012, 24 PVC chambers (10 cm diameter, 0.86 L average volume) were installed 10 cm into the soil of the experimental plots and remained in place for the entire winter (Figure 2-2). An open piece of tubing was installed next to the chambers to measure ambient CO_2 under the snowpack. To eliminate disturbance of the snowpack, this tubing, along with tubing from the chambers, extended to an off-plot location. During sampling, the CO_2 concentration in the snowpack was determined using a Li-820 infrared gas analyzer (LI-COR Biosciences, Lincoln, NE, USA; hereafter

referred to as IRGA). The CO_2 concentration within the chamber was then measured and scrubbed down to the ambient snowpack concentration using soda lime, at which point flux measurement began. Air was circulated between the chamber and the IRGA at 1L min^{-1} and the CO_2 concentration was recorded every 2 seconds. The flux calculation is described in detail in the appendix. All chamber measurements (n=152 on control and warming plots) were performed in low wind (< 8 mps) conditions.

Snow Pit Measurements

Because the CiPEHR experimental design requires an undisturbed snowpack to maintain the warming treatment, we established separate plots in the fall of 2009 at a nearby off-experiment location (~100 m away) to measure R_{eco} using the snow-pit method (e.g. Elberling, 2007; Morgner *et al.*, 2010). At the snow-pit site, we installed forty PVC bases (25.4 cm diameter, 10 cm into soil, 12.8 L average chamber volume) in sets of four. Each set of four was adjacent to an individual soil temperature and soil moisture probe (n=10). A snow pit was dug to uncover the base prior to each sampling effort. This snow removal prior to sampling eliminates issues of diffusivity through the snowpack that must be accounted for when measuring directly on top of the snow. Snow was left in the base and snow density was measured to account for this change in volume. The snow pits ranged from 3 to 100 cm in depth, depending on the plot and time of year. We waited 20 minutes after removing snow to allow the CO_2 to equilibrate between the soil and snow before placing the chamber on the base (Vogel *et al.*, 2009). Once the chamber was placed on the base, we circulated the air through an IRGA and the chamber at 1L min^{-1}, recording the CO_2 concentration every 1 second for 2 minutes (Figure 2-2). After sampling, the pit was re-filled with snow. The set of four bases were re-measured sequentially over the winter so that each sampling effort did not use the

previously uncovered bases; this reduced the impact of snow removal-related disturbance to the plots. Snow pit measurements (n=826) were taken in 2009, 2011, 2012, and 2013.

Eddy Covariance

CO_2 exchange during the snow-covered period was also measured using eddy covariance (EC) at a location approximately 1 km west of CiPEHR from 2008 though 2013 (Figure 2-2). The EC system consisted of a Campbell Scientific CSAT3 (Campbell Sci Inc. Logan, UT, USA) sonic anemometer and a Li-COR Li-7500 open path CO_2/H_2O gas analyzer (LI-COR Biosciences, Lincoln, NE, USA) mounted on a 3.5 m tower. Data were recorded at a frequency of 10 Hz on a Campbell Scientific CR5000 data logger and fluxes were Reynolds averaged over 30 min time periods (Reynolds, 1985). CO_2 fluxes were corrected for variations in air density due to fluctuation in water vapor and heat fluxes (Webb *et al.*, 1980) and for fluctuations caused by surface heat exchange from the open path sensor during wintertime conditions (Burba *et al.*, 2008). The tower footprint was greater than 400 m in all directions and consisted of vegetation similar to that found at CiPEHR. Belshe *et al.* (2012) provide more details of EC flux processing at this site.

Soda Lime

Winter R_{eco} at CiPEHR was also measured by soda lime adsorption (e.g.Grogan & Chapin, 1999b; Nobrega & Grogan, 2007; Rogers *et al.*, 2011). Prior to placing soda lime at the CiPEHR plots, we weighed 300g of 4-8 mesh soda lime into 1L mason jars and dried for 24 hours at 100°C. Immediately after removing from the drying oven, mason jars were capped and stored until deployment. Bottomless 5 gallon buckets were inserted 15cm into the ground on the control and warming plots (n=12 per

treatment). In late September, we added 100-150 ml of water to each Mason jar to increase the adsorption capacity of the soda lime and placed one open jar inside each bucket, which was immediately capped for the entirety of the winter (Figure 2-2). We also deployed 6 mason jars into capped buckets with the bottom still intact as blanks such that the soda lime was not exposed to the soil or the atmosphere. In late April (2010-2012) or May (2013), the mason jars were collected from the field and immediately capped. The soda lime was then dried for 240 hours at 100°C and 24 hours at 75°C. R_{eco} was determined by the change in soda lime dry weight, corrected for water loss associated with adsorption (Grogan, 1998).

Fall Chamber Flux

To capture CO_2 flux dynamics in the fall before photosynthesis had stopped for the year, static chamber measurements were made on the CiPEHR plots in the fall of 2009, 2011, 2012, and 2013. Fluxes were measured on the warming and control plots by circulating air through a plexi-glass chamber and an IRGA. At each plot, both light and dark (achieved with chamber cover) fluxes were performed to estimate NEE and $R_{eco.}$ Fluxes from all three years (n=588) were combined into one data set for light (photosyntheically active radiation, PAR>10 μE) and dark fluxes. In 2013, it was determined that photosynthesis had stopped before static flux measurements began (no significant difference between light and dark fluxes, mixed effects ANOVA, $p>0.4$), so light measurements were not included in analysis.

Radiocarbon

To determine how the relative contribution of old C to R_{eco} changed by season, natural abundance of $\Delta^{14}C$ and $\delta^{13}C$ were measured from the on-plot chambers

installed at CiPEHR (n=6 per treatment) in April of 2012 and 2013. These R_{eco} isotopes were also measured at CiPEHR in August of the same years from 12 permanent PVC collars fixed 8 cm in the soil. Detailed methods of radiocarbon field collection and lab processing are available in Schuur *et al.* (2009). $\Delta^{14}C$ values were corrected for residual atmospheric CO_2 using the $\delta^{13}C$ values in a 2-pool mixing model as described by Schuur and Trumbore (2006). These corrected values were then normalized by the atmospheric $\Delta^{14}C$ value for 2012 to compare between years.

Field Environmental Measurements

In 2012-2013, snow depth was measured on the control and winter warming side of one snow fence every three hours using a Campbell Scientific SR50A sonic ranging senor (Campbell Sci In. Logan, UT, USA). Snow depth at the snow pit plots was measured before sampling using a 1 m ruler. Soil moisture and temperature sensors were located were within 1 m of each on-plot and snow pit flux plot. Volumetric water content (hereafter referred to as soil moisture) was measured as an integrated value from the soil surface to 20 cm depth using site-calibrated Campbell Scientific CS616 water content reflectometer probes. Soil temperature was measured using constantan-copper thermocouples at 5, 10, 20, and 40 cm. Soil moisture and temperature were recorded every thirty minutes using Campbell Scientific CR1000 data loggers (Campbell Sci Inc. Logan, UT, USA). An Onset HOBO (Onset Computer Corporation, Bourne, MA, USA) weather station located approximately 100 m from the experimental plots recorded PAR, and air temperature and pressure every two minutes. Active layer depth was measured using a metal depth probe in September at each winter flux location.

Statistical Analysis

Seasonal Definitions

We defined *winter* as the period when the photosynthetic flux is not significantly different from zero. This is different from the point at which NEE is negative (net C uptake), as photosynthesis may still be occurring despite a net loss of C when R_{eco} losses are greater than photosynthetic gain. Because there was limited data from clear chamber measurements directly on the CiPEHR plots, we used spring and fall EC data to define the threshold when photosynthesis stopped in the fall and started in the spring. To determine when photosynthesis was active, we used a one-sided t-test to test when light (PAR>10 μE) fluxes from the EC tower were significantly ($p<0.05$ without the Bonferroi correction) more negative than nighttime (PAR<10 μE) fluxes. Because the data were not continuous in all years, we compared the population of light fluxes to the population of dark fluxes within a five-day moving window and then applied the Bonferroni correction to account for multiple comparisons. In years with insufficient EC data, the most reasonable estimates of seasonal change were used based on the average of all other years or on available data. In the fall of 2010, our data showed some C uptake until DOY 323 but after that point there is a gap in the data. All statistical analyses were conducted using R version 2.15.1 (R Core Development Team, 2012).

At the CiPEHR experiment, the growing season has previously been defined as the period between May 1st and September 30th (*Natali et al.*, 2011, *Natali et al.*, 2014). By defining the growing season by the same number of calendar days every year, it is possible to determine whether differences in C fluxes across years are due to changes in ecosystem processes (such as greater summertime R_{eco}) rather than changes in

season length (such as a later onset of a fall). Here we define the weeks after September 30th but before photosynthesis had reached the minimum threshold for the year as *fall*. The months before April 30th when photosynthesis was above the minimum, threshold we call *spring.* The period between September 30th and April 30th, which comprises fall, winter, and spring, we call the *non-growing season* (NGS).

Analysis of the Environmental Drivers of Winter CO_2 Flux

To determine the drivers of winter CO_2 flux, we constructed a separate model for each of the three flux methods with temporal resolution: on-plot chamber measurements, snow pit chamber measurements, and EC. In all cases, the response variable (ecosystem CO_2 flux) was log transformed. Variance inflation factors were used to determine which explanatory variables were collinear and should not be included in the analysis (values with a variance inflation factor over three were not used, as suggested by *Zuur et al.*, 2009). Explanatory variables considered were: wind speed, atmospheric pressure, air temperature, soil temperature, and day of season (DOS). Snow depth, active layer depth, and treatment (on-plot only) were also included in the initial snow pit and on-plot models, but snow depth was too highly correlated with the remaining variables in the snow pit model, so it was excluded from further analysis. The first DOS was defined as October 1st in all years and the season extended until April 30th.

For the two chamber measurements, we used mixed effects models using the lme command in the nlme package in R (Pinherio *et al.*, 2013) with multiple environmental variables as the fixed effects and experimental design (nested: block, snow fence, plot for on-plot measurements and nested: plot, subplot for the snow pit method) as the random effects. For the EC model, we used the lm function in the base

package in R and there were no random effects. The best model for each measurement method was selected using the lowest *Akaike information criterion (AIC)* and the residuals of all final models were checked for normality and homogeneity of variances.

Modeling Wintertime R_{eco}

We determined CO_2 loss during the winter using a non-linear multiple regression model (separate models were created for the on-plot, snow pit, and EC methods). Because our goal was to model biological CO_2 production (R_{eco}) and not CO_2 flux, which results from both biological and physical processes, we chose a model based only on the biological drivers of winter R_{eco}. We described winter CO_2 loss as follows:

$$R_{eco} = \alpha * e^{\beta 1 * T + \beta 2 * DOS}$$

where α is the basal respiration rate, β1 is the rate of respiration change per degree T (soil temperature), and β2 is the rate of change per DOS. Alpha (α) varied by the random effects. Analysis of all methods, including full and biological models, is provided in the appendix.

We estimated CO_2 loss during all winters (2008-2009 through 2012-2013) including those during which we had no flux measurements (2008-2009; 2010-2011) by using the model to predict CO_2 loss based on measured environmental variables at CiPEHR. Carbon loss was predicted at each of the 24 CiPEHR plots and each of these plot predictions was averaged by treatment per experimental fence and then by treatment to calculate total amount of C lost from the experiment during the winter. Standard error was calculated using snow fence (n=6) as the level of replication.

Modeling Fall NEE

The CO_2 balance during the fall was determined using response functions from measured R_{eco} and NEE. R_{eco} was modeled separately for the control and warming treatment using the nlme function in the R nlme package (Pinherio *et al.*, 2013) using the equation:

$$R_{eco}=\alpha*e^{\beta T}$$

where α is the basal respiration rate, β is the rate of respiration change and T is the soil temperature. To incorporate repeated measures, α was allowed to vary by the nested random effects: experimental block, fence, and plot. NEE was also modeled separately for the control and warming treatment using the nlme function and the equation:

$$NEE = [(\alpha*PAR*F_{max})/(\alpha*PAR+F_{max})]+R_d$$

where α is the initial linear slope of the light response curve, F_{max} is the maximum photosynthesis at light saturation, PAR is photosynthetically active radiation at the time of measurement, and R_d is dark ecosystem respiration. Again, R_d was allowed to vary by the nested random effects: experimental block, fence, and plot. Parameter values for these functions are reported in Table 2-2.

Modeling Spring NEE

We used the EC data to determine the spring photosynthetic uptake as a proportion of average summertime GPP such that γ = (average GPP in spring)/(average GPP during the first two weeks of May). Because we were unable to measure NEE at CiPEHR in the spring (we could only measure R_{eco}), we applied this proportion γ to each of the plots (n=12 per treatment) at CiPEHR such that such that spring NEE= R_{eco} (winter modeled, above)-γ*(average measured GPP from the first two weeks in May). Average measured GPP during the first two weeks of May was calculated on an

individual plot basis based on data collected from automated chambers deployed during the growing season (Natali *et al.* 2011). In 2013, there were no autochamber measurements from 2013, so flux values from 2012 were used. In the spring of 2010 and 2013 we did not have sufficient data to calculate γ from the EC tower, so we applied the average value of γ obtained in 2009, 2011, and 2012.

Total NGS C Balance

The NGS CO_2 balance was calculated by adding the NEE estimates from spring and fall to the winter R_{eco} estimate. As with the winter CO_2 balance, error was calculated using snow fence as the level of replication and describes the spatial error of this estimate.

Table 2-1. Average soil temperature, snow depth, air temperature, and atmospheric pressure measured at CiPEHR during the October-April of 2008-2013. Soil temperature is the average of 5, 10, 20, and 40 cm depths. In all years, the treatment effect on soil temperature was significant ($p<0.001$). Spring snow depth was measured before the shoveling effort each spring (see methods). Snow depth was measured in mid-March in 2009, early April in 2013, and mid-April in 2010-2012. Values in parenthesis are the spatial standard error of the estimate.

Non-growing season	Average soil temperature (°C)			Spring snow depth (cm)		Average air temperature (°C)	Average atmospheric pressure (atm)
	Control	Warming	Treatment difference	Control	Warming		
2008-2009	-2.8 (0.3)	-1.2 (0.2)	1.6 (0.3)	39 (3)	130 (1)	-12.92	0.92*
2009-2010	-4.2 (0.2)	-2.9 (0.2)	1.2 (0.3)	17 (2)	75 (1)	-9.24	0.92*
2010-2011	-3.8 (0.2)	-1.5 (0.2)	2.3 (0.3)	23 (1)	103 (3)	-11.07	0.92*
2011-2012	-2.6 (0.4)	-1.0 (0.1)	1.5 (0.3)	55 (3)	118 (2)	-10.68	0.91
2012-2013	-1.5 (0.3)	-0.9 (0.2)	0.6 (0.5)	66 (1)	119 (2)	-12.83	0.92

* Indicates missing data from the on-site weather station during this year. Values are filled from nearby weather station.

Table 2-2. Mean estimate and standard error of parameters for the control and warming fall NEE and R_{eco} (μmol m^{-2} s^{-1}) models.

Model	Coefficient	Treatment	Mean estimate	SE
Reco	Basal respiration (α)	Control	0.41	0.03
		Warming	0.57	0.08
	Rate of respiration change (β)	Control	0.18	0.06
		Warming	0.43	0.06
NEE	Maximum photosynthesis ($F_{max)}$	Control	-1.46	1.79
		Warming	-3.88	8.28
	Initial linear slope (α)	Control	-1.18E-03	6.75E-04
		Warming	-1.57E-03	7.90E-04
	Dark ecosystem respiration (R_d)	Control	0.35	0.06
		Warming	0.46	0.09

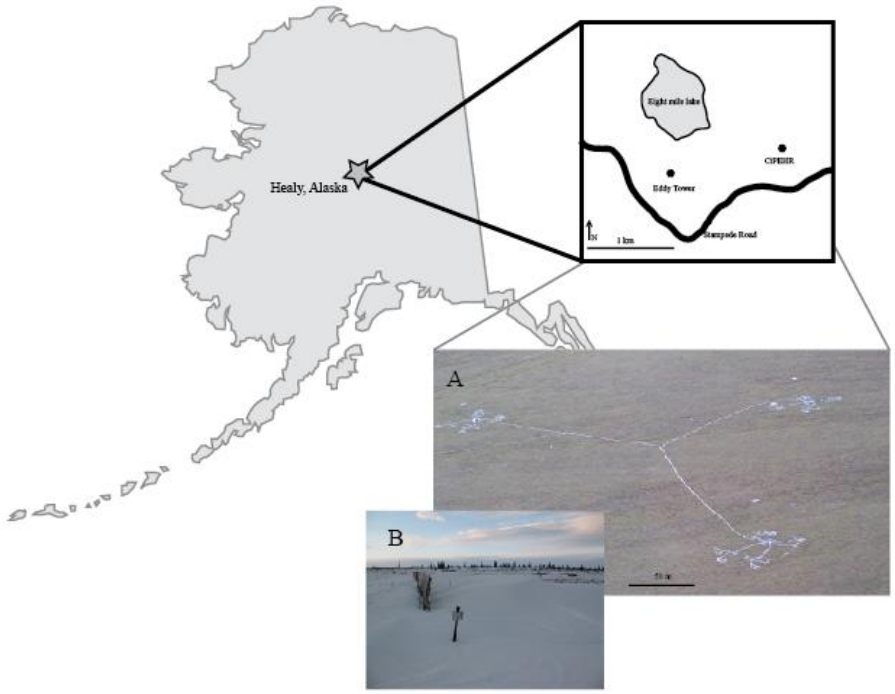

Figure 2-1. Location of CiPEHR, eddy covariance tower, and the Eight Mile Lake region within the context of Alaska. A) An aerial photograph of CiPEHR during the growing season. Note the three experimental blocks. B) Within each experimental block are two snow fences. Photographs courtesy of Elizabeth E. Webb.

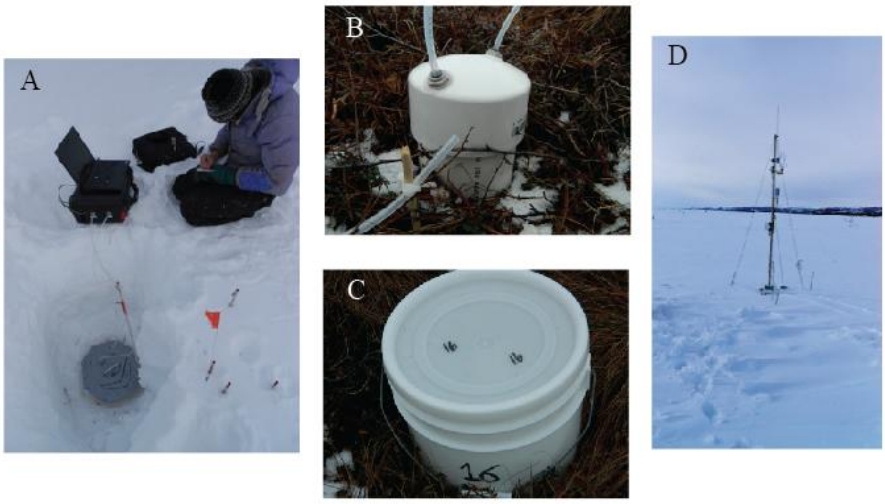

Figure 2-2. Photographs of the four methods of measuring winter CO_2 flux. A) Snow pit B) On-plot C) Soda lime D) Eddy covariance. Photographs courtesy of Elizabeth E. Webb.

CHAPTER 3
RESULTS

Method Comparison

To compare between methods, we modeled cumulative R_{eco} during the winter of 2012-2013 based on each of the three (EC, snow pit, on-plot) measurement-derived models and the biologically relevant variables (day of season and soil temperature) measured at the CiPEHR control plots during this time period (Table 3-1). The mean of all measurement methods was 107.5 g CO_2-C m^{-2} $winter^{-1}$. There was more than a two-fold difference between methods (Figure 3-1), with EC estimating the highest amount of CO_2 (45% higher than the mean of all methods). The on-plot chamber measurements showed the lowest amount of CO_2 loss, estimating 39% lower than the mean of all methods. Soda lime, which measures the cumulative amount of CO_2 adsorbed and is not modeled, was higher than the two chamber measurements, which were most similar to each other.

The trend observed in method differences for measuring winter CO_2 flux was preserved in NGS C loss estimates; NGS estimates made with the chamber models were lower than for soda lime adsorption (which was measured, not modeled) and EC (Table 3-2). Yet while EC estimated the highest NGS C loss, it showed the lowest difference (9%) between the control and warming treatment when the model was applied to both sets of measured temperatures. In contrast, soda lime showed the greatest difference between control and warming (average 36% increase). The on-plot method was next highest, at an average increase of 32%, and the snow pit showed a 14% increase between the control and warming treatments over five years.

The range of estimated cumulative CO_2 loss between measurement methods was a direct result of differences in measured fluxes, as all models were run on the same soil temperatures and season length for comparison. The on-plot chambers were only sampled during 2012-2013, the winter with the warmest soil temperatures (Table 2-1), and as such we do not have measurements below -4.5 °C (Figure 3-2). Despite sampling exclusively during the warmest winter, the on-plot chambers measured the lowest average flux of the three methods (0.34 vs. 0.43 and 0.82 μmol CO_2 m^{-2} s^{-1} for the snow pit and EC methods, respectively). The on-plot measurements also had the least variability between fluxes, even when compared with the other two methods at soil temperatures greater than -4.5 °C. However, the medians of the on-plot and snow pit measurements were very close (0.28 vs 0.32 μmol CO_2 m^{-2} s^{-1}) whereas the median of the EC measurements was much larger (0.55 μmol CO_2 m^{-2} s^{-1}). In addition to the highest average flux, the EC also had the lowest and highest measurements, which is likely a result of the high temporal coverage of this dataset compared to the other methods. When measurements taken on the same day under similar environmental conditions (low wind, equivalent soil temperatures) were compared, the snow pit and EC were not significantly different ($p=0.1$; mixed effects repeated measures ANOVA). It is likely, however, that the reduced number of measurements observed during these times (snow pit n=196; EC n=164) was not sufficient to detect a difference and a type II error occurred. The on-plot and EC measurements were significantly different ($p=0.001$) when compared during the same day.

Drivers of Winter CO_2 Flux

The three models derived separately from snow pit, on-plot, and EC measurements quantify the relationship between CO_2 flux and possible covariates.

These models identify the drivers of winter CO_2 flux as soil temperature, DOS, atmospheric pressure, air temperature, and the interaction between pressure and air temperature. With the exception of DOS in the on-plot model and soil temperature in the EC model, all factors were significant ($p<0.05$) in all three models (Table 3-3). It is well documented that soil temperature is an important driver in soil respiration and thus we kept soil temperature in the EC model. It is likely that the relationship between soil temperature and flux is weak in the EC model because EC calculates flux at the landscape level, whereas soil temperature was measured at one point near the tower. In all models, wind speed, snow depth, active layer depth, and experimental treatment were not significant ($p>0.05$).

The relationship between CO_2 flux and DOS was negative, meaning that holding all other covariates constant, CO_2 flux decreased throughout the winter. The relationship between CO_2 flux and soil temperatures was positive; in all models higher soil temperatures increased CO_2 flux, all other covariates being equal (Table 3-1; Table 3-3). Of all the soil depths measured (5, 10, 20, 40 cm, and the average of these depths), we found soil temperature at 10 cm to be the best predictor of winter R_{eco}. Air temperature, atmospheric pressure, and the interaction between the two were also significant drivers of winter CO_2 flux, likely because both impact the process of gas diffusion from the soil to the atmosphere. All gas diffusion is driven in part by atmospheric pressure, and CO_2 movement is also governed by air temperature via advection. These two effects were magnified at low air temperatures and low atmospheric pressures.

Seasonal Variation

The onset of winter (end of detectable plant C uptake) varied as much as 55 days over the five years measured (Figure 3-3, Table 3-4) whereas the end of winter (start of plant C uptake) was much more stable, varying only by 11 days despite the drastically different snow conditions during the five winters (Table 2-1). This means the period of the year during which there is no photosynthesis varied as much as 49 days, and this variation was driven almost entirely by when photosynthesis stops in the late fall. We were unable to attribute the end or beginning of photosynthesis to environmental variables such as a temperature or moisture thresholds.

As determined by EC measurements, photosynthetic C uptake in the spring was 7, 13, and 30% of the C uptake in mid-May in 2009, 2010, and 2011, respectively. This value, γ, is the percentage we used to estimate CO_2 uptake under the snowpack on the CiPEHR plots. The temperature sensitivity of R_{eco} also varied between the growing season and the NGS (Figure 3-4). Wintertime C fluxes were systematically over-estimated by the temperature response curve fit to both growing season and NGS R_{eco} fluxes, indicating that Q_{10} is not constant throughout the year. Additionally, the $\Delta^{14}C$ signature of R_{eco} changed between the growing season and the end of winter; it was significantly lower in April than in August (Figure 3-5; $p=0.02$). The $\Delta^{14}C$ values, however, were not affected by year ($p=0.6$) or by treatment ($p=0.9$).

Non-Growing Season C Balance

While we calculated NGS CO_2 loss estimates using all four methods (Table 3-2), we proceeded with the snow pit method for NGS CO_2 loss analysis because it estimated a moderate amount of CO_2 loss (of all the methods tested, it did not predict the smallest or largest amount of CO_2 released; Table 3-2), had a sufficient number of

measurements (n=826) to capture yearly and seasonal variation, and has been well tested in the existing literature.

Despite frigid temperatures, the sheer length of the winter season meant that CO_2 loss during the NGS was driven mostly by the winter (81%) with small contributions from the fall (10%) and the spring (8%; values in parenthesis are averaged over treatment and years; Figure 3-6). In all years, the warming treatment lost more CO_2 than the control in the fall (p=0.009; one sided paired t-test) and the winter (p=0.002; paired one sided t-test) whereas in the spring, the warming treatment did not show a difference in C loss (p=0.2;paired one sided t-test), as higher R_{eco} was offset by greater plant uptake. The warming treatment lost, on average 26% more CO_2 in the fall and 15% more CO_2 in the winter.

Total NGS CO_2 loss was between 68 and 93 g CO_2-C m^{-2} $season^{-1}$ for the control and 82 and 99 g CO_2-C m^{-2} $season^{-1}$ for the warming treatment (Figure 3-6; Table 3-2). Experimental warming increased NGS C loss (p=0.002; paired one-sided t-test) on average by 14%, but this percent increase varied from 7 to 24%, depending on the year. Differences in inter-annual NGS C loss were primarily due to variation in soil temperatures (Figure 3-7; p= 0.001; mixed effects ANOVA), though years with the longest winters showed the greatest C loss over the entire NGS (p=0.1; mixed effects ANOVA). Overall, NGS CO_2 loss was exponentially related to soil temperature (Figure 3-7).

We next modeled NGS CO_2 loss assuming R_{eco} was the only ecosystem CO_2 flux only from October-April (i.e. there is no photosynthesis during the snow-covered period) and compared this estimate to our method of incorporating GPP during the spring and

fall. On average, the R_{eco}-only method estimated 12% more C loss than the GPP-sensitive method (Figure 3-8). However, this difference was more pronounced for the control than for the warming treatment ($p=0.007$; repeated measures mixed effects ANOVA). This suggests that, based on our method of modeling fall and spring GPP, warming stimulated R_{eco} more than GPP during the NGS.

Table 3-1. Mean estimate and standard error of parameters for the on-plot, snow pit, and eddy covariance biological winter CO2 flux (µmol m-2 s-1) models. Day of season was not significant in the on-plot model.

Method	Coefficient					
	Basal respiration (α)		Soil temperature at 10cm (β1)		Day of season (β2)	
	Mean estimate	SE	Mean estimate	SE	Mean estimate	SE
On-plot	0.53	0.092	0.250	0.053	-	-
Snow pit	0.67	0.041	0.094	0.022	-0.0027	4.9E-04
Eddy covariance	1.05	0.066	0.056	0.026	-7.6E-04	7.5E-04

Table 3-2. Total non-growing season CO_2 loss estimates (g CO_2-C m^{-2}) for the 5 years of soil temperature and PAR data available at CiPEHR. The on-plot, snow pit, and eddy covariance estimates are modeled based on fall and method-specific winter, and spring parameters. The soda lime was measured directly on the plots and the estimate was scaled to the same number of days (October 1- April 30) in all years. Values in parenthesis are the spatial standard error of the estimate.

Method	Year									
	2008-2009		2009-2010		2010-2011		2011-2012		2012-2013	
	Control	Warming	Control	Warming	Control	Warming	Control	Warming	Control	Warming
On-plot	66 (3)	80 (3)*	47 (1)	60 (1)*	48 (1)	73 (2)*	54 (4)	77 (2)*	78 (4)	91 (4)*
Snow pit	89 (2)	97 (1)*	71 (1)	82 (0.3)*	68 (1)	84 (1)*	74 (2)	86 (1)*	93 (2)	99 (2)*
Eddy covariance	182 (2)	193 (2)*	152 (1)	166 (0.4)*	136 (1)	158 (1)*	157 (3)	173 (1)*	186 (2)	194 (2)*
Soda lime	-	-	-	-	136 (31)	159 (35)	120 (24)	205 (28)*	148 (19)	176 (22)

*Indicates that the warming treatment released significantly ($p<0.05$; one-sided t-test) more CO_2 than the control for this method in this year.

Table 3-3. Mean estimate and standard error of parameters from the full on-plot, snow pit, and EC winter CO_2 flux (μmol CO_2 m^{-2} s^{-1}) models. Normalized estimates are a way to compare the relative importance of variables but should not be used in prediction. The numbers in parenthesis represent the rank order of variable importance within each model. While there is debate in the statistics community about the validity of p-values from parameter estimates of mixed effects models, we report p-values here, as is common in ecology, as a way to measure signal strength on a common scale. The EC model is a multiple linear regression with fixed effects only and thus has a p-value whereas the on-plot and snow removal models are mixed effects models and do not have p-values. R^2 values for the mixed effects models were calculated after *Nakagawa and Schielzeth*, 2013. Results are shown for the best-fit models only.

Coefficient		Method		
		On-plot	Snow pit	Eddy covariance
Intercept	Mean estimate	24.19	-0.48	10.98
	SE	7.74	3.81	4.70
	P-value	0.002	0.901	0.020
	Normalized estimate	1.80	1.81	-0.70
Atmospheric pressure	Mean estimate	-23.69	0.10	-12.49
	SE	8.40	4.12	5.17
	P-value	0.006	0.981	0.016
	Normalized estimate	0.07	0.10	0.03
Air temperature	Mean estimate	3.68	1.73	1.30
	SE	0.84	0.35	0.34
	P-value	<0.001	<0.001	<0.001
	Normalized estimate	0.11	0.10	0.03
Day of season	Mean estimate	-	-0.006	-0.002
	SE	-	0.00	0.00
	P-value	-	<0.001	0.012
	Normalized estimate	-	-0.48	-0.12 (2)
Soil temperature (10 cm)	Mean estimate	0.19	0.09	0.01
	SE	0.06	0.02	0.03
	P-value	0.004	<0.001	0.686
	Normalized estimate	0.21 (2)	0.21	0.02 (3)
Atmospheric temperature	Mean estimate	-3.96	-1.87	-1.42
x Air temperature	SE	0.91	0.38	0.38
	P-value	<0.001	<0.001	<0.001
	Normalized estimate	-0.26 (1)	-0.15	-0.12 (1)
Model R^2	Fixed effects only	0.21	0.36	0.03
	Fixed and random effects	0.46	0.52	NA
Model p-value		NA	NA	<0.001

Table 3-4. Winter season (period of no photosynthesis) length and start and end dates for the 5 years measured.

Winter	Season length (days)	Start		End	
		DOY	Date	DOY	Date
2008-2009	183	270	29-Sep	88*	25-Mar
2009-2010	158	295*	14-Oct	88*	26-Mar
2010-2011	134	325*	21-Nov	94	30-Mar
2011-2012	148	300	29-Oct	83	23-Mar
2012-2013	168	283	11-Oct	86	26-Mar

* Indicates there was not enough EC data from this year to determine start or end date and instead the most reasonable estimate based on available data was used.

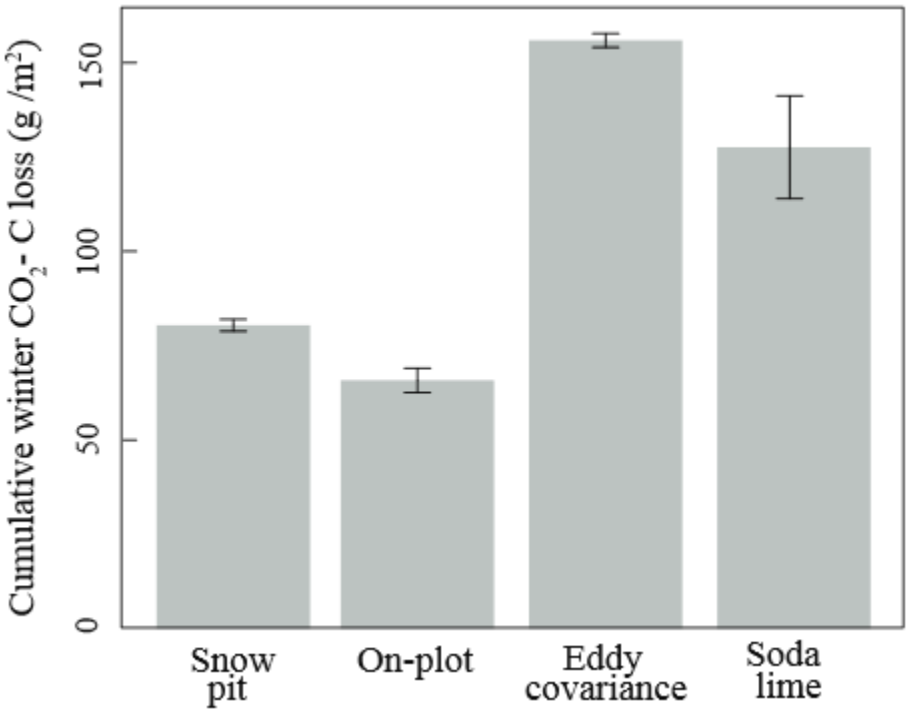

Figure 3-1. Winter 2012-2013 CO_2 loss measured using the soda lime technique and modeled using the snow pit, on-plot, and eddy covariance (EC) biological models. All models were applied to soil temperature measured at the CiPEHR control plots. Since the soda lime was left on the plots for the entire NGS but here we show a comparison of winter CO_2 loss, the soda lime measurement was scaled by the number of days during the winter. Error bars represent standard error of spatial variation. All estimates were significantly different from each other ($p<0.05$; Tukey's post-hoc test) except the snow pit and on-plot methods.

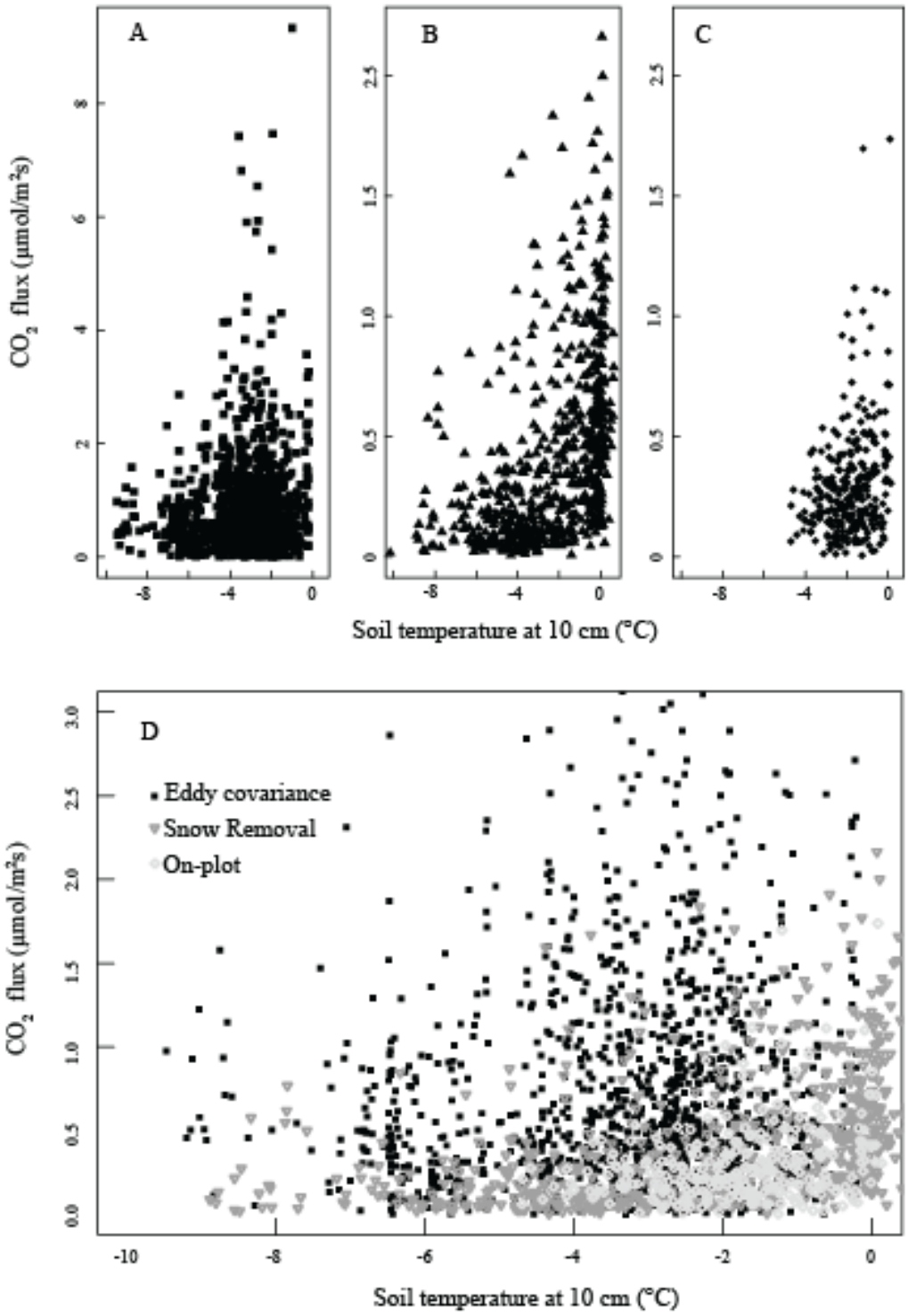

Figure 3-2. Winter CO_2 flux as measured by the three methods used to create flux models. A) Eddy covariance (EC) B) Snow pit C) On-plot. Note the difference in y-axis scales. D) All methods plotted on the same y-axis; some EC measurements have been cut off for comparison.

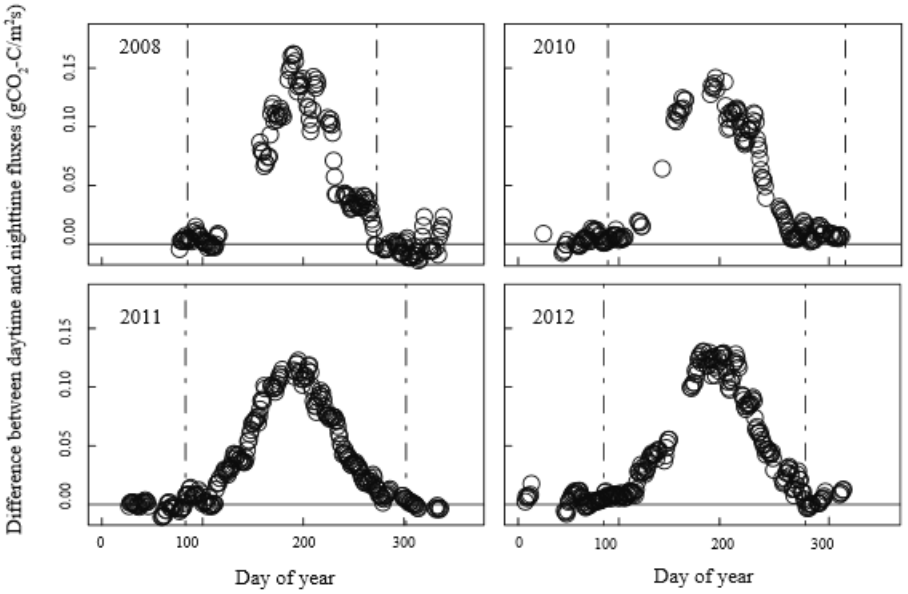

Figure 3-3. The seasonal differences between daytime (PAR>10 µE) and nighttime (PAR<10 µE) NEE in four representative years using a 5-day moving window for EC fluxes. Dashed lines represent start and end of photosynthesis for each year as determined by a one-sided t-test.

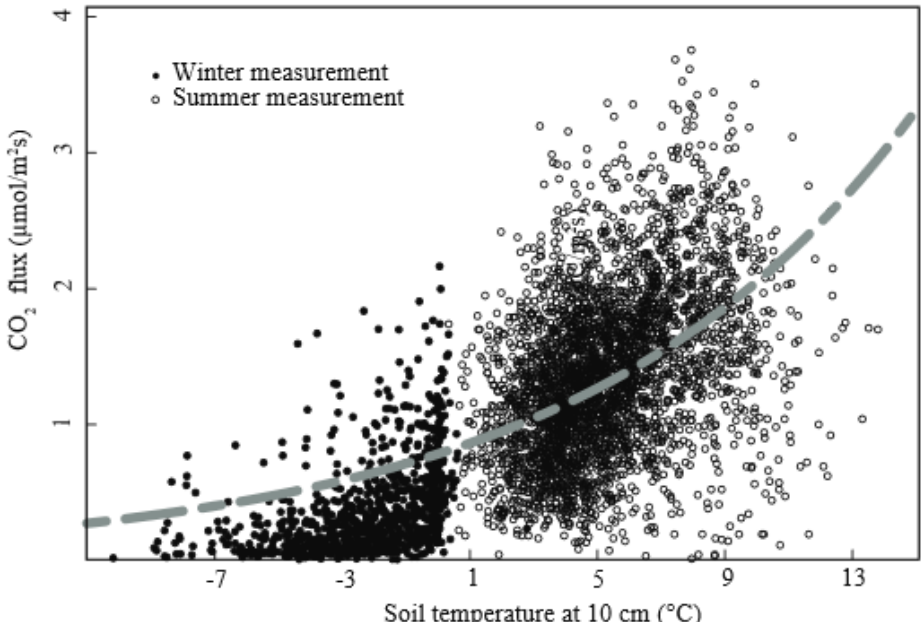

Figure 3-4. Winter (snow pit and on-plot) and summer R_{eco} fluxes (control and warming, May- September 2008) plotted against soil temperature. Eddy data was excluded from this figure to compare chamber measurements between seasons. The dashed line represents the best-fit exponential curve through all the data points. Information about methods of collecting summer flux measurements is provided in Natali et al. 2011.)

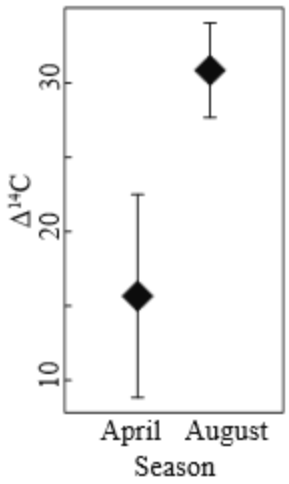

Figure 3-5. Delta (Δ) 14C (‰) from R_{eco} measured at control and warmed plots at CiPEHR during April and August of 2012 and 2013. Delta 14C varied by season (p=0.01) but not by year (p=0.5) or treatment (p=0.9). Smaller values reflect longer residence time of C, indicating an increased contribution of old C to R_{eco}.

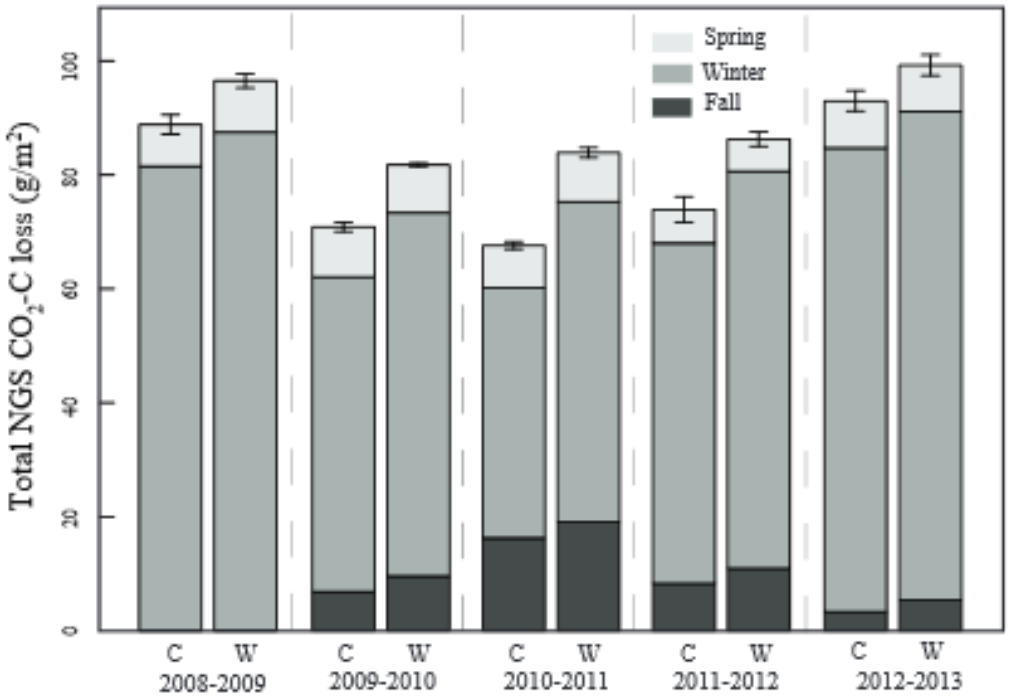

Figure 3-6. Total NGS CO_2 loss for the control (C) and warming (W) treatment partitioned by season (fall, winter, spring) for the five years of temperature and PAR data available at CiPEHR. Total NGS CO_2 loss was calculated using the snow pit biological model for winter and spring respiration. Standard error bars represent the spatial error for the total NGS estimate. In all years, warming released significantly more CO_2 during the NGS than control ($p<0.02$).

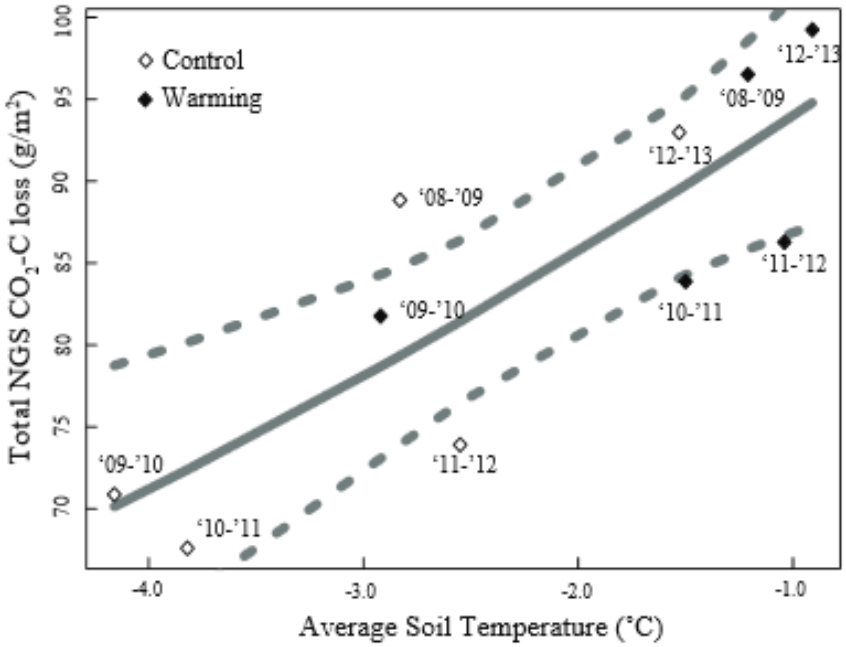

Figure 3-7. Total NGS CO_2 loss as a function of October-April average soil temperature (10 cm). Each point represents the modeled CO_2 loss of the control or warming treatment during one NGS. The solid line is the best-fit exponential model ($\alpha*\exp(\beta T)$) of the data and the dashed lines represent the model 95% confidence intervals. Here α=103.1and β=0.09; both parameters are significant ($p<0.003$). The Q_{10} of this function is 2.5.

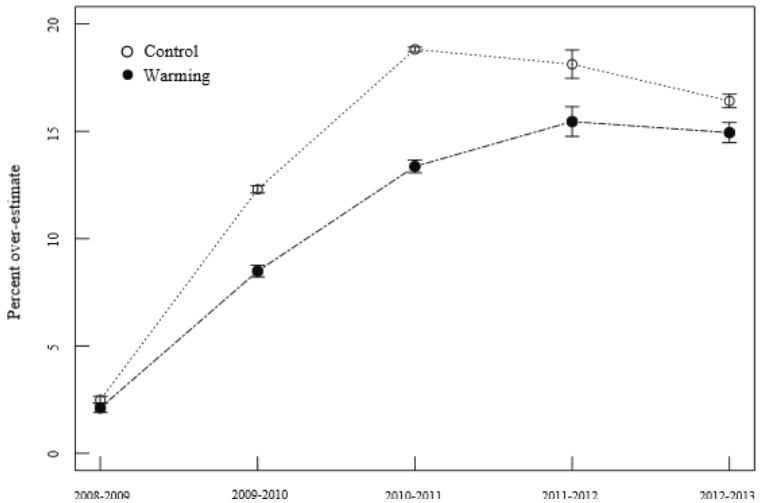

Figure 3-8. Percent by which assuming only R_{eco} occurs during the NGS over estimates NGS CO2 loss. The percent increase grew over time ($p<0.001$; repeated measures mixed effects ANOVA) and was more pronounced in the control than in the warming treatment ($p=0.007$). Standard error bars represent the spatial error of the estimate.

CHAPTER 4
DISCUSSION

Comparison of Measurement Methods

While winter respiration plays a pivotal role in the annual C balance in the arctic, there is large uncertainty in winter C budgets because of methodological limitations of measuring fluxes in arctic winter field conditions. Our study, which aimed to reduce this uncertainty through a methods comparison, found that for a single field site, there was a four-fold range in NGS C loss across the four methods employed. However, these measurements constrained NGS C flux (between 47 and 186 g CO_2-C m^{-2} $season^{-1}$ for the control) at the mid to high end of the published arctic tundra winter respiration estimates (0.19 to 210 g CO_2-C m^{-2} $season^{-1}$ over a similar time period; converted units from Björkman *et al.*, 2010a).

In contrast with other studies that showed the highest rates of CO_2 flux from chambers placed over the soil as opposed to diffusion methods or chambers placed directly on the snow (Björkman *et al.*, 2010a), we found that chamber methods measured the lowest CO_2 flux of the four methods tested (Figure 3-1). Because chamber methods must only be employed during low wind conditions (Bain *et al.*, 2005), and because more CO_2 is released in windy conditions as a result of snow and soil venting (Bowling & Massman, 2011), extrapolating fluxes during low wind conditions to the entire winter may underestimate the amount of C released. In contrast, EC is able to capture soil and snow venting events because it measures during turbulent conditions. Indeed, while wind speed was not a significant control of CO_2 flux in any of our models, Euskirchen *et al.* (2012) found that wind speed was an important driver of winter CO_2 flux in tundra ecosystems using EC towers. It is possible that the EC

method employed in this study overestimated total CO_2 lost by extrapolating measurements from high wind conditions to times of no wind. However we found that even in times of low wind (< 8 mps), the EC tower measured fluxes higher than the two chamber methods (p=0.001 for on-plot and p=0.1 for snow pit).

In this study, the soda lime adsorption method showed higher cumulative winter CO_2 loss than the two chamber measurements. Soda lime may over estimate C loss by drawing down CO_2 in the bucket headspace, thus creating a gradient where CO_2 diffuses out of the soil at a higher rate than under natural conditions (Nay *et al.*, 1994; Grogan & Chapin, 1999; Nobrega & Grogan, 2007). Indeed, Nay *et al.* (1994) found that at low rates of CO_2 flux, soda lime over-estimated the expected flux by 25%. Nobrega and Grogan (2011) noted that this effect can be decreased by installing the chambers deep in the soil (10cm), thus isolating the soil volume affected. Our buckets were installed 15cm into the ground, yet when we measured the CO_2 concentration of the bucket headspace immediately before removing the soda lime jars from the field in the spring of 2013, we found concentrations below ambient CO_2 levels (the average bucket was 125 ppm above the ambient concentration; data not shown). This indicated that after eight months in the field, the soda lime appeared to be drawing down the bucket headspace CO_2 concentration, potentially resulting in an overestimated CO_2 flux.

Drivers of Winter CO_2 Flux

Soil temperature is a primary driver of soil respiration due to the temperature sensitivity of microbial enzymes (Davidson & Janssens, 2006) and the effect of temperature on available water in solution (Clein & Schimel, 1995; Tilston *et al.*, 2010). Additionally, it is well established that winter R_{eco} in tundra soils results from biological activity rather than from diffusion of stored CO_2 in the soils (Zimov *et al.*, 1996; Panikov

et al., 2006). The temperature sensitivity of microbial decomposition (Q_{10}; Q_{10} is the change in R_{eco} for a 10°C temperature increase) in frozen soils, however, is less well understood; the range of Q_{10} values reported in the literature is between 1 and 237 for winter arctic soils (Mikan *et al.*, 2002; Elberling & Brandt, 2003; Panikov *et al.*, 2006; Elberling, 2007; Morgner *et al.*, 2010; Euskirchen *et al.*, 2012, Natali *et al.,* 2014, Oechel *et al.,* 2014), although most values are between 2 and 13 (when the Q_{10} was not published, we calculated the value based on the reported exponential curve parmaters; Elberling & Brandt, 2003; Panikov *et al.*, 2006; Morgner *et al.*, 2010; Euskirchen *et al.*, 2012; Natali et al. in press; Oechel *et al.* 2014). Our Q_{10} values are on the lower end of this spread (12.2 for on-plot, 2.6 for snow pit, and 1.8 for EC), which is, at least in part, due to the fact that soil temperature is not the only explanatory variable in our (snow pit and EC) models. Other studies that quantify the relationship between C flux and soil temperature with additional explanatory variables (such as wind speed, pressure, or net radiation) also report lower values (Euskirchen *et al.*, 2012; Oechel *et al.*, 2014). These lower Q_{10} values (~1-13) are more in the range of values published for terrestrial soils (Lenton & Huntingford, 2003; Hamdi *et al.*, 2013), but it is understood that, in general, Q_{10} increases at lower temperatures (Lloyd & Taylor, 1994; Davidson & Janssens, 2006).

Elberling & Brandt (2003) and Elberling (2007) found that there was no evidence for a shift in temperature sensitivity around 0°C and that a single Q_{10} value could be applied to the same soil at all temperatures. In contrast, Schuur *et al.* (2009) argued for a biological threshold around 0°C and applied different temperature response curves to measurements above and below 0°C. In general this has been the approach of most

studies, which analyze CO_2 flux data from the growing season separately from the NGS (e.g. Welker *et al.*, 2000; Vogel *et al.*, 2009; Euskirchen *et al.*, 2012; Natali *et al.* 2014). We found that when a single Q_{10} value was applied to measurements from both the growing season and the winter, the winter was systematically over-estimated (Figure 3-4). This supports the system of partitioning the year into the growing season and the NGS. However, because growing season R_{eco} measurements comprise both plant and soil processes whereas winter R_{eco} is, for the most part, a result of heterotrophic respiration, we cannot decipher whether the Q_{10} of soil respiration itself changes over the course of the year.

In addition to soil temperature, we found that DOS is a biological driver (contributing to CO_2 *production* rather than diffusion out of the soil) of winter C flux, with more C released at the beginning of the season than at the end when all other conditions are similar. This phenomenon of a change in the magnitude of C flux over the winter season has also been documented by others (Zimov *et al.* 1996; Oechel *et al.*, 1997; Fahnestock *et al.*, 1999; Morgner *et al.*, 2010), although in some cases a spring surge in C release was also observed (Zimov *et al.*, 1996; Oechel *et al.*, 1997; Fahnestock *et al.*, 1999). It is not known whether this spring surge is physical (CO_2 that was trapped in the soils is released upon thaw; Elberling & Brandt, 2003) or biological (nutrients from dead microbial biomass is released upon thaw, stimulating decomposition from freeze-tolerant microbes; Skogland *et al.*, 1988; Schimel & Clein, 1996). We did not observe a burst in R_{eco} in the spring, although less than one percent of our data were collected when soil temperatures were above 0°C in the spring (Figure 3-2).

The heightened C loss early in the winter is most often attributed to the relatively warmer soil temperatures and greater amount of unfrozen water present in the soils at this time (Oechel *et al.*, 1997; Fahnestock *et al.*, 1999). However, our models indicated that DOS decreased over the course of the winter even when soil temperature was held constant. We hypothesize that the larger CO_2 release early in the season to the presence of recently senesced plant inputs, which are easily decomposable and dominate the available C pool. Later in the season, this pool decreases, leading to declines in CO_2 flux rates. Indeed, it is thought that winter R_{eco} in the arctic is derived primarily from recent labile plant inputs as opposed to bulk soil C (Grogan *et al.*, 2001; Grogan, 2012). In a meta-analysis of high latitude soil incubation studies, Schädel et al. (2014) established that the labile C pool of permafrost soils is exhausted after ~150 days at 5 °C, after which the microbial community shifts to a reliance on more slowly decomposing C. While 5 °C is warmer than the average temperature of winter tundra soils, it is likely that after 7 months without any new plant inputs, there is much less labile C in our soils than at the start of winter. Schimel et al. (2004) measured nitrogen mineralization in tundra soils in the fall (Sept-Nov) and during the winter (Nov-March or Nov-May) and found nitrogen mineralization rates were higher during the winter than in the fall, indicating microbes are more C limited by the end of the winter than in the fall. Additionally, ^{14}C data from our field site and from boreal soils (Winston *et al.*, 1997) show a ^{14}C signature for R_{eco} that is more negative at the end of the winter than it is mid-summer (Figure 3-5), indicating that by the end of the winter, microbes are decomposing a greater proportion of older, and often more slowly decomposing C (Trumbore & Czimczik, 2008; Schmidt *et al.*, 2011). It is also possible that the

seasonal difference in the R_{eco} ^{14}C signature is due to increased plant respiration in the summer as opposed to April.

An additional hypothesis for our observed C flux decrease over the course of the winter is that in the early part of the winter, there is unfrozen water in soil pores but as the season progresses, this water freezes and is thus unavailable to microbes. Hence, there would be more C released at the beginning of the season, when the soils are freezing as opposed to at the same temperatures in the spring before the soils have thawed. This hypothesis is supported by microbial ecology; microbes need liquid water for respiration, extracellular enzyme movement, and substrate diffusion (Clein & Schimel, 1995; Mikan *et al.*, 2002). Panikov *et al.* (2006) and Tilston *et al.* (2010) showed that in the laboratory, frozen soil C flux was related to both water content and temperature. However, field studies of moisture control have remained elusive and, at least in one study, summertime moisture levels did not affect winter flux (Elberling, 2007). We opted not to use moisture as a covariate in our analysis due to uncertainty about the sensor calibrations during the frozen period (Pers. communication with Campbell Scientific, 2013). However, a simple regression between the raw millivolt output of our moisture probes and winter C flux showed decreased flux with increasing resistance (more moisture). Including the raw millivolt output from our moisture probes in the models did not eliminate DOS as a significant predictor of CO_2 flux. This suggests that ice may actually be restricting CO_2 diffusion out of the soil, which has also been documented in frozen soils laboratory experiments (Elberling & Brandt, 2003). In this circumstance, the effect of the frozen water is to act as a physical barrier to CO_2 diffusion but that does not exclude the possibility that the unfrozen water content is

simultaneously limiting biological CO_2 production. Thus, while water may limit microbial activity in frozen soils, it may also limit CO_2 diffusion out of the soil, making it challenging to isolate the effect of moisture on CO_2 flux in the field.

While many studies have shown a positive correlation between snow depth and winter CO_2 flux (e.g. Fahnestock *et al.*, 1998, 1999; Jones *et al.*, 1999; Nobrega & Grogan, 2007; Rogers *et al.*, 2011), snow depth was not a significant contributor to winter C release in any of our models. This could be because studies that point to snow depth as an important driver measured C flux at plots that span a range of snow depths at a few times throughout the year. In contrast, we sampled the same plots as they accumulated snow over the winter. Because our measurements spanned many years and include data of different snow depths in the same plot, we tracked intra-plot as well as inter-plot response to snow depth. While (snow pit) plots with higher average snow depth did show more C release, snow depth was too highly correlated with other variables to be used on our modeling analysis. However, when CO_2 flux was regressed against snow depth alone, there was a negative relationship. Euskirchen *et al.* (2012) also found a negative relationship between snow depth and winter CO_2 flux using EC towers, which they attribute to CO_2 trapping in the snowpack. Since our chamber measurements were made directly over the soil instead of over the snowpack, it is unlikely that CO_2 trapping within the snowpack was the cause of this negative relationship. Instead, snow depth was highly correlated with DOS and soil temperature, indicating that the negative relationship between CO_2 flux and snow depth was because there is a negative relationship with soil temperature and DOS. Hence, while snow

plays an important role in insulating the soil from the cold winter air temperatures, it is soil temperature and DOS that is driving CO_2 flux.

Non-Growing Season C Balance

Uncovering the mechanisms underlying NGS C cycling and quantifying NGS C loss is critical to understanding the Arctic's ability to act as a C sink. To quantify NGS CO_2 loss, we first partitioned the NGS into the times when photosynthesis was active or dormant. This approach is more rigorous than previous definitions of winter (Grogan & Jonasson, 2006, *Natali et al.*, 2014, Oechel *et al. 2014*) because it incorporates inter-annual variability and accounts for plant C uptake even when snow is present. Our fall and winter CO_2 loss values are estimated based on measurement-derived models and environmental variables measured directly at the CiPEHR plots. Similarly, the spring R_{eco} values are also based on a measurement-derived model and soil temperature measured directly at CiPEHR whereas the spring GPP estimates were made based on a percentage, as determined by EC tower measurements, of CO_2 flux measurements made at the plots in May. We found that seasonal variation led to estimates that were 12% lower than when we modeled NGS CO_2 loss by assuming that R_{eco} is the only ecosystem process during the NGS (Figure 3-8). This evaluation might be an underestimate, however, because both the spring and the fall seasons are expected to lengthen with climate change (Euskirchen *et al.*, 2009; Christensen *et al.*, 2013b).

Next we quantified NGS C loss by modeling NEE based on environmental variables, rather than applying an average rate to the entire season or interpolating between points (e.g. Oechel *et al.*, 1997; Welker *et al.*, 2000; Björkman *et al.*, 2010b). We used DOS and soil temperature to model R_{eco} during the winter and spring, improving upon other models that only used soil temperature to quantify winter C loss

(Elberling, 2007; Morgner *et al.*, 2010; Natali *et al.*, 2014). Research conducted in March and April of 2009 at our study site showed a 28% increase in basal respiration in response to warming (Natali *et al.*, 2014), however we did not observe this pattern during the years of our study. Instead we found that the warming treatment was not a significant ($p>0.05$) predictor of winter CO_2 flux in the on-plot model, indicating that experimental warming did not influence CO_2 flux aside from its effect on temperature. In other words, our study found that the warming treatment released more CO_2 because of increased soil temperature rather than because of the additive effects of increased basal respiration and increased soil temperature. We attribute these contrasting results to different methodological approaches.

Similar to other studies (Welker *et al.*, 2000; Nobrega & Grogan, 2007; Morgner *et al.*, 2010; Natali *et al.*, 2014), our results show that the warming treatment lost more C over the NGS than the control (Figure 3-6). The soda lime method indicated that warming increased CO_2 loss by an average of 36%, but the variation was high enough such that this effect as only significant in 2011-2012 (Table 3-2). Across the other three methods, the warming treatment released significantly more CO_2 in all years (on average 32 % (on-plot), 14% (snow pit), and 9 % (EC) more). Thus, even though soil temperature was not the only predictor of NGS CO_2 loss, our data demonstrate that as the winter climate warms, CO_2 loss during the NGS could increase exponentially (Figure 3-7). Additionally, CO_2 loss during the NGS was driven mostly by the winter (Figure 3-6) with small contributions from the fall and the spring, indicating that NGS CO_2 loss will be further magnified with climate warming, since the greatest temperature increases are expected in December-February (Christensen *et al.*, 2013a).

To understand the annual C balance of the tundra, the warming-induced increase in NGS CO_2 loss must be put in the context of the growing season, where experimental warming increased R_{eco} at the same site by 18, 24, and 46 % across the study years, 2009, 2010, and 2011(Natali *et al.*, 2014). When combined with growing season NEE at the same site, our results show that the tundra was, on average, a CO_2 source in both the control and warming plots for the three years (2009, 2010, 2011) of growing season data available (Natali *et al.*, 2014). Depending on the method used to calculate NGS CO_2 loss, the control plots lost, on average, 27 (on-plot, SE=17), 49 (snow pit; SE=18), and 129 (EC; SE=25) g CO_2-C m^{-2} yr^{-1}. Annual CO_2 loss for the warming plots was 22 (on-plot; SE=33), 38 (snow pit; SE=34), 123 (EC; SE=40) g CO_2-C m^{-2} yr^{-1} (estimates are the average and SE of annual CO_2 loss by method for the first three years of the experiment).

It has long been speculated that C loss over the winter period could shift the tundra from a C sink to a source, but lack of data precluded many substantive studies. While we only have three years of data, our results support multiple lines of evidence from individual field studies (Oechel *et al.*, 1993; Welker *et al.*, 2000; Natali *et al*. 2014), a meta-analysis of field studies (Belshe *et al.*, 2013), and modeling simulations that indicate that the tundra is shifting from the historical C sink to a C source (Koven *et al.*, 2011; Schneider von Deimling *et al.*, 2012). These results highlight the great importance of considering both the growing and non-growing season contributions to annual CO_2 flux from arctic ecosystems and the importance of refining our understanding of climate change driven changes in soil temperature, seasonal patterns, and the mechanisms driving ecosystem C loss.

APPENDIX
SUPPLEMENTARY MATERIAL

On-plot Chamber Measurement Flux Calculation

The on-plot chambers were sampled according to the following method: 1.) The CO_2 concentration of the snow pack was measured. 2.) CO_2 free air was run through the chamber until the chamber concentration matched that of the ambient snow pack. 3.) Unaltered air was circulated between the IRGA and the chamber headspace for fifteen minutes. We found that it took longer to bring the chamber headspace to the ambient snow pack CO_2 concentration than would be expected from the 1 L min^{-1} flow rate of the IRGA pump. We attributed this to the fact that the chamber headspace is not a closed system and so as the CO_2 concentration within the chamber decreased, CO_2 stored in the soil diffused into the chamber headspace. Indeed, after scrubbing stopped, we saw an initial spike in the rate of CO_2 accumulation (Figure A-1) that can be explained by rapid CO_2 diffusion from the soil to the chamber as a result of the altered diffusion gradient. We also saw this initial sharp increase when we tested this method on a closed chamber installed in sand. Because there was no biological flux from the sand, we can be sure this initial rise in CO_2 concentration is the result of physical processes. Thus, it is important to not include this high rate of CO_2 diffusion in the flux calculation.

However, at some point the perturbation-related diffusion into the chamber will end and CO_2 will diffuse out of the soil at the same rate as under the surrounding snowpack. When the headspace concentration increases enough, CO_2 will diffuse out of the chamber or laterally through the soil instead of vertically into the chamber. The problem we faced was knowing when we were measuring diffusion that was occurring

at the same rate as the surrounding snow pack, or when CO_2 diffusion into the chamber was increasing linearly. In other words, the point at which the first derivative of the CO_2 concentration vs. time curve is linear should be the point at which perturbation-related diffusion stopped but before CO_2 diffusion out of the chamber started. To determine this point, we took the second derivative of the CO_2 concentration vs. time curve. We then recorded the first derivative at the point where the second derivative was zero. We tested this method of data processing against laboratory tests on a CO_2 flux generator (Martin *et al.*, 2004) and field tests during the summer when we could remove the chamber top.

Winter CO_2 Flux Models

We created multiple-regression (for EC) and mixed effects (for the chamber methods) models to determine the drivers of winter CO_2 flux. We found that DOS, soil temperature, air temperature, atmospheric pressure, and the interaction between air temperature and atmospheric pressure were significant controls over winter CO_2 flux (Table 3-3). However, because our sampling was not frequent enough to capture all physical aspects of CO_2 flux such as snow pack venting events, we chose to model CO_2 *production* over the winter, which is dependent only on biological controls: DOS and soil temperature.

We compared the outcome of the biology-only models with the full models (DOS, soil temperature, air temperature, atmospheric pressure, and the interaction between air temperature and atmospheric pressure) of each measurement technique (Figure A-2). The EC full model was consistently higher than the EC biological model and the difference between the two models varied between 8 and 25 %, depending on the year. For the chamber models, the pattern was not consistent; in some years the biological

model predicted higher CO_2 loss than the full model, but in other years this trend was reversed. The difference between the full and biological models varied between 2 and 18 % for the chamber models. The trend of the on-plot method predicting the lowest CO_2 loss and the EC predicting the highest CO_2 loss was preserved in all models and years. The difference between the full and biological models is small and all values lie well within the range of published winter tundra CO_2 loss estimates (Björkman *et al.*, 2010a). Additionally, the lack of consistent directionality in the difference between the full and biological models suggests that we are not systematically biasing our calculations by predicting winter CO_2 loss with the biology-only models.

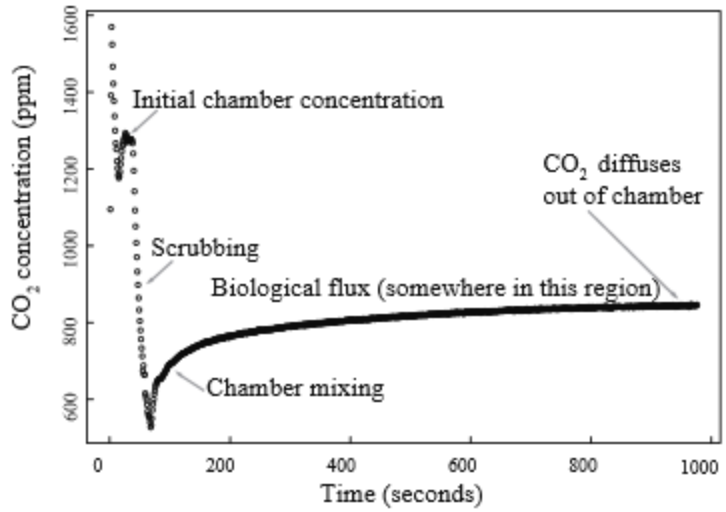

Figure A-1. Representative example of the CO_2 concentration vs. time curve for the on-plot chamber measurements. After CO_2 free air is run through the chamber, there is an initial sharp increase in slope that is the result of diffusion and not a biological flux. After this rapid flow into the chamber has stopped, there is a biological flux before the chamber concentration increases enough so that CO_2 diffuses out of the chamber.

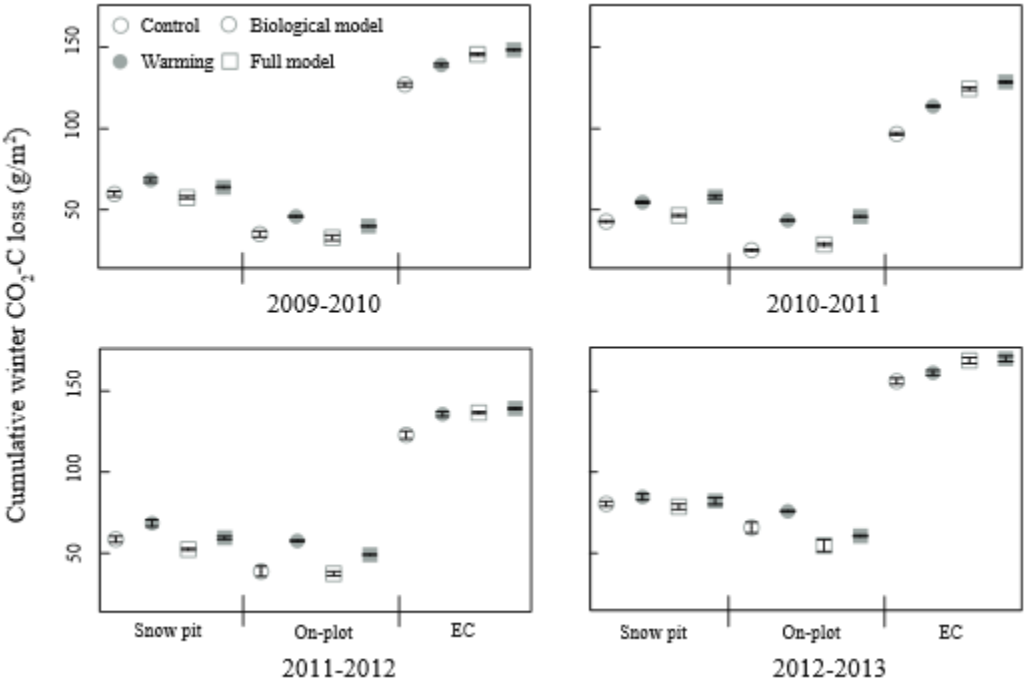

Figure A-2. Comparison between the full and biological models used to predict wintertime CO_2 loss. Estimates are for the control and warming treatments in four representative years. EC model was applied to soil temperatures measured at CiPEHR plots.

LIST OF REFERENCES

Bain WG, Hutyra L, Patterson DC, Bright A V, Daube BC, Munger JW, Wofsy SC (2005) Wind-induced error in the measurement of soil respiration using closed dynamic chambers. *Agricultural and Forest Meteorology*, **131**, 225–232.

Belshe EF, Schuur EAG, Bolker BM, Bracho R (2012) Incorporating spatial heterogeneity created by permafrost thaw into a landscape carbon estimate. *Journal of Geophysical Research*, **117**, 1–14.

Belshe EF, Schuur EAG, Bolker BM (2013) Tundra ecosystems observed to be CO_2 sources due to differential amplification of the carbon cycle. *Ecology letters*, 1307–1315.

Biasi C, Meyer H, Rusalimova O et al. (2008) Initial effects of experimental warming on carbon exchange rates, plant growth and microbial dynamics of a lichen-rich dwarf shrub tundra in Siberia. *Plant and Soil*, **307**, 191–205.

Björkman MP, Morgner E, Cooper EJ, Elberling B, Klemedtsson L, Björk RG (2010a) Winter carbon dioxide effluxes from Arctic ecosystems: An overview and comparison of methodologies. *Global Biogeochemical Cycles*, **24**.

Björkman MP, Morgner E, Björk RG, Cooper EJ, Elberling B, Klemedtsson L (2010b) A comparison of annual and seasonal carbon dioxide effluxes between sub-Arctic Sweden and High-Arctic Svalbard. *Polar Research*, **29**, 75–84.

Bowling DR, Massman WJ (2011) Persistent wind-induced enhancement of diffusive CO_2 transport in a mountain forest snowpack. *Journal of Geophysical Research*, **116**, G04006.

Burba GG, McDdermitt DK, Grelle A, Anderson DJ, Xu L (2008) Addressing the influence of instrument surface heat exchange on the measurements of CO_2 flux from open-path gas analyzers. *Global Change Biology*, **14**, 1854–1876.

Campbell Scientific (2013) Personal Communication.

Christensen JH, Kumar KK, Aldrian E et al. (2013a) Climate Phenomena and their Relevance for Future Regional Climate Change. In: *Climate Change 2013: The Physical Science Basis. Contribution of Working Group 1 to the fifth Assessment Report of the Intergovernmental Panel on Climate Change* (eds Stocker T., Qin D, Plattner G-K, Tignor M, Allen SK, Boschung J, Nauels A, Xia Y, Bex V, Midgley PM). Cambridge University Press, Cambridge, United Kingdom and New York, NY, USA.

Christensen JH, Kumar KK, Aldrian E et al. (2013b) Long-term Climate Change: Projections, Commitments and Irreversibility. In: *Climate Change 2013: The Physical Science Basis. Contribution of Working Group 1 to the fifth Assessment Report of the Intergovernmental Panel on Climate Change* (eds Stocker T., Qin D, Plattner G-K, Tignor M, Allen SK, Boschung J, Nauels A, Xia Y, Bex V, Midgley PM). Cambridge University Press, Cambridge, United Kingdom and New York, NY, USA.

Clein JS, Schimel JP (1995) Microbial activity of tundra and taiga soils at sub-zero Ttemperatures. *Soil Biology and Biochemistry*, **27**, 1231–1234.

Davidson EA, Janssens IA (2006) Temperature sensitivity of soil carbon decomposition and feedbacks to climate change. *Nature*, **440**, 165–73.

Elberling B (2007) Annual soil CO_2 effluxes in the High Arctic: The role of snow thickness and vegetation type. *Soil Biology and Biochemistry*, **39**, 646–654.

Elberling B, Brandt KK (2003) Uncoupling of microbial CO_2 production and release in frozen soil and its implications for field studies of arctic C cycling. *Soil Biology and Biochemistry*, **35**, 263–272.

Euskirchen ES, McGuire A. D, Rupp TS, Chapin FS, Walsh JE (2009) Projected changes in atmospheric heating due to changes in fire disturbance and the snow season in the western Arctic, 2003–2100. *Journal of Geophysical Research*, **114**, G04022.

Euskirchen ES, Bret-Harte MS, Scott GJ, Edgar C, Shaver GR (2012) Seasonal patterns of carbon dioxide and water fluxes in three representative tundra ecosystems in northern Alaska. *Ecosphere*, **3**.

Fahnestock JT, Jones MH, Brooks PD, Walker DA, Welker JM (1998) Winter and early spring CO_2 efflux from tundra communities of northern Alaska. *Journal of Geophysical Research*, **103**, 23–27.

Fahnestock JT, Jones H, Welker M (1999) Wintertime CO_2 : efflux from arctic soils : Implications for annual carbon budgets. *Global Biogeochemical Cycles*, **13**, 775–779.

Grogan P (1998) CO_2 flux measurement using soda lime : correction for water formed during CO_2 adsorption. *Ecology*, **79**, 1467–1468.

Grogan P (2012) Cold season respiration across a low arctic landscape : the influence of vegetation type , snow depth , and interannual climatic variation. *Arctic, Antarctic, and Alpine Research*, **44**, 446–456.

Grogan P, Chapin FS (1999) Arctic soil respiration : effects of climate and vegetation depend on season. *Ecosystems*, **2**, 451–459.

Grogan P, Jonasson S (2006) Ecosystem CO_2 production during winter in a Swedish subarctic region: the relative importance of climate and vegetation type. *Global Change Biology*, **12**, 1479–1495.

Grogan P, Illeris L, Michelsen A, Jonasson S (2001) Respiration of recently-fixed plant carbon dominates mid-winter ecosystem CO_2 production in sub-arctic heath tundra. *Climactic Change*, 129–142.

Hamdi S, Moyano F, Sall S, Bernoux M, Chevallier T (2013) Synthesis analysis of the temperature sensitivity of soil respiration from laboratory studies in relation to incubation methods and soil conditions. *Soil Biology and Biochemistry*, **58**, 115–126.

Harden JW, Sundquist ET, Stallard RF, Mark RK (1992) Dynamics of soil carbon during deglaciation of the laurentide ice sheet. *Science*, **258**, 1921–1924.

Hicks Pries CE, Schuur EAG, Crummer KG (2011) Holocene carbon stocks and carbon accumulation rates altered in soils undergoing permafrost thaw. *Ecosystems*, **15**, 162–173.

Hicks Pries CE, Schuur E a. G, Vogel JG, Natali SM (2013) Moisture drives surface decomposition in thawing tundra. *Journal of Geophysical Research: Biogeosciences*, **118**.

Hobbie SE, Schimel JP, Trumbore SE, Randerson JR (2000) Controls over carbon storage and turnover in high-latitude soils. *Global Change Biology*, **6**, 196–210.

Huemmrich KF, Kinoshita G, Gamon JA, Houston S, Kwon H, Oechel WC (2010) Tundra carbon balance under varying temperature and moisture regimes. *Journal of Geophysical Research*, **115**, G00I02.

Jones MH, Fahnestock JT, Welker JM (1999) Early and late winter CO_2 efflux from arctic tundra in the Kuparuk river watershed, Alaska, U.S.A. *Arctic, Antarctic, and Alpine Research*.

Kappen L (1993) Plant activity under snow and ice, with particular reference to lichens. *Arctic*, **46**, 297–302.

Koven CD, Ringeval B, Friedlingstein P et al. (2011) Permafrost carbon-climate feedbacks accelerate global warming. *Proceedings of the National Academy of Sciences of the United States of America*, **108**, 14769–74.

Lee H, Schuur E a. G, Vogel JG, Lavoie M, Bhadra D, Staudhammer CL (2011) A spatially explicit analysis to extrapolate carbon fluxes in upland tundra where permafrost is thawing. *Global Change Biology*, **17**, 1379–1393.

Lenton TM, Huntingford C (2003) Global terrestrial carbon storage and uncertainties in its temperature sensitivity examined with a simple model. *Global Change Biology*, **9**, 1333–1352.

Lloyd J, Taylor JA (1994) On the temperature dependence of soil respiration. *Functional Ecology*, **8**, 315–323.

Martin JG, Bolstad P V, Norman JM (2004) A carbon dioxide flux generator for testing infrared gas analyzer-based soil respiration systems. *Soil Science Society of America Journal*, **68**, 514–518.

Mikan CJ, Schimel JP, Doyle AP (2002) Temperature controls of microbial respiration in arctic tundra soils above and below freezing. *Soil Biology and Biochemistry*, **34**, 1785–1795.

Morgner E, Elberling B, Strebel D, Cooper EJ (2010) The importance of winter in annual ecosystem respiration in the High Arctic: effects of snow depth in two vegetation types. *Polar Research*, **29**, 58–74.

Nakagawa S, Schielzeth H (2013) A general and simple method for obtaining R^2 from generalized linear mixed-effects models (ed O'Hara RB). *Methods in Ecology and Evolution*, **4**, 133–142.

Natali SM, Schuur EAG, Trucco C, Hicks Pries CE, Crummer KG, Baron Lopez AF (2011) Effects of experimental warming of air, soil and permafrost on carbon balance in Alaskan tundra. *Global Change Biology*, **17**, 1394–1407.

Natali SM, Schuur EAG, Rubin RL (2012) Increased plant productivity in Alaskan tundra as a result of experimental warming of soil and permafrost. *Journal of Ecology*, **100**, 488–498.

Natali SM, Schuur EAG, Webb EE, Hicks Pries CE, Crummer KG (2014) Permafrost degradation stimulates carbon loss from experimentally warmed tundra. *Ecology*.

Nay MS, Mattson KG, Bormann BT (1994) Biases of chamber wethods for measuring soil CO_2 efflux demonstrated with a laboratory apparatus. *Ecology*, **75**, 2460–2463.

Nobrega S, Grogan P (2007) Deeper snow enhances winter resipration from both plant-associated and bulk soil carbon pools in birch hummock tundra. *Ecosystems*, **10**, 419–431.

Oberbauer SF, Tweedie CE, Welker JM et al. (2007) Tundra CO_2 fluxes in response to experimental warming across latitudinal and moisture gradients. *Ecological Monographs*, 221–238.

Oechel WC, Hastings SJ, Vourlitis G, Jenkins M, Riechers G, Grulke N (1993) Recent change of Arctic tundra ecosystems from a net carbon dioxide sink to a source. *Nature*, **361**, 9–12.

Oechel WC, Vourlitis G, Hastings SJ (1997) Cold Season CO_2 emissions from arctic soils. *Global Biogeochemical Cycles*, **11**, 163–172.

Oechel WC, Vourlitis G, Hastings S, Zulueta R, Hinzman L, Kane D (2000) Acclimation of ecosystem CO2 exchange in the Alaskan Arctic in response to decadal climate warming. *Nature*, **406**, 978–81.

Oechel WC, Laskowski CA, Burba G, Gioli B, Kalhori, AAM (2014) Annual patterns and budget of CO_2 flux in an arctic tussock tundra ecosystem. *Journal of Geophysical Research.*

Osterkamp TE, Jorgenson MT, Schuur EAG, Shur YL, Kanevskiy MZ, Vogel JG (2009) Physical and ecological changes associated with warming permafrost and thermokarst in interior Alaska. *Permafrost and Periglacial Processes*, **256**, 235–256.

Panikov NS, Flanagan PW, Oechel WC, Mastepanov M a., Christensen TR (2006) Microbial activity in soils frozen to below −39°C. *Soil Biology and Biochemistry*, **38**, 785–794.

Pinherio J, Bates D, Saikat D, Sarkar D (2013) nlme: Linear and nonlinear mixed effects models. R package. *R-core*.

R Core Development Team (2012) R: A language and environment for statistical computing.

Reynolds O (1985) On the dynanmical theory of incompressible viscous fluids and the determination of the criterion. *Philosophical transactions of the Royal Society of London. Series A*, **186**, 123–164.

Rogers MC, Sullivan PF, Welker JM (2011) Evidence of nonlinearity in the response of net ecosystem CO_2 exchange to Iincreasing levels of winter snow depth in the high arctic of northwest Greenland. *Arctic, Antarctic, and Alpine Research*, **43**, 95–106.

Rustad LE, Campbel JL, Marion GM et al. (2001) A meta-analysis of the response of soil respiration, net nitrogen mineralization, and aboveground plant growth to experimental ecosystem warming. *Oecologia*, **126**, 543–562.

Schädel C, Schuur EAG, Bracho R et al. (2014) Circumpolar assessment of permafrost C quality and its vulnerability over time using long-term incubation data. *Global change biology*, **20**, 641–52.

Schimel JP, Clein JS (1996) Microbial response to freeze-thaw cycles in tundra and taiga soils. *Soil Biol. Biochem*, **28**, 1061–1066.

Schimel JP, Bilbrough C, Welker JM (2004) Increased snow depth affects microbial activity and nitrogen mineralization in two Arctic tundra communities. *Soil Biology and Biochemistry*.

Schmidt MWI, Torn MS, Abiven S et al. (2011) Persistence of soil organic matter as an ecosystem property. *Nature*, **478**, 49–56.

Schneider von Deimling T, Meinshausen M, Levermann A, Huber V, Frieler K, Lawrence DM, Brovkin V (2012) Estimating the near-surface permafrost-carbon feedback on global warming. *Biogeosciences*, **9**, 649–665.

Schuur EAG, Trumbore SE (2006) Partitioning sources of soil respiration in boreal black spruce forest using radiocarbon. *Global Change Biology*, **12**, 165–176.

Schuur EAG, Crummer KG, Vogel JG, Mack MC (2007) Plant species composition and productivity following permafrost thaw and thermokarst in Alaskan tundra. *Ecosystems*, **10**, 280–292.

Schuur EAG, Bockheim J, Canadell JG et al. (2008) Vulnerability of permafrost carbon to climate change: implications for the global carbon cycle. *BioScience*, **58**, 701.

Schuur EAG, Vogel JG, Crummer KG, Lee H, Sickman JO, Osterkamp TE (2009) The effect of permafrost thaw on old carbon release and net carbon exchange from tundra. *Nature*, **459**, 556–9.

Schuur EAG, Abbott BW, Bowden WB et al. (2013) Expert assessment of vulnerability of permafrost carbon to climate change. *Climatic Change*, **119**, 359–374.

Shaver GR, Billings WD, Chapin FS, Giblin AE, Nadelhoffer KJ, Oechel WC, Rastetter EB (1992) Global change and the carbon Bbalance of arctic ecosystems. *BioScience*, **42**, 433–441.

Sistla SA, Moore JC, Simpson RT, Gough L, Shaver GR, Schimel JP (2013) Long-term warming restructures Arctic tundra without changing net soil carbon storage. *Nature*, 1–5.

Sjögersten S, van der Wal R, Woodin SJ (2008) Habitat type determines herbivory controls over CO_2 fluxes in a warmer Arctic. *Ecology*, **89**, 2103–16.

Skogland T, Lomeland S, Goksoyr J (1988) Respiratory burst after freezing and thawing of soil: experiments with soil bacteria. *Soil Biology and Biochemistry*, **20**.

Starr G, Oberbauer SF (2003) Photosynthesis of arctic evergreens under snow: implications for tundra ecosystem carbon balance. *Ecology*, **84**, 1415–1420.

Sullivan PF, Welker JM, Arens SJT, Sveinbjörnsson B (2008) Continuous estimates of CO_2 efflux from arctic and boreal soils during the snow-covered season in Alaska. *Journal of Geophysical Research*, **113**.

Tarnocai C, Canadell JG, Schuur E a. G, Kuhry P, Mazhitova G, Zimov S (2009) Soil organic carbon pools in the northern circumpolar permafrost region. *Global Biogeochemical Cycles*, **23**.

Tieszen LL (1974) Photosynthetic competence of the subnivean vegetation of an arctic tundra. *Arctic and Alpine Research*, **6**, 253–256.

Tilston EL, Sparrman T, Öquist MG (2010) Unfrozen water content moderates temperature dependence of sub-zero microbial respiration. *Soil Biology and Biochemistry*, **42**, 1396–1407.

Trucco C, Schuur EAG, Natali SM, Belshe EF, Bracho R, Vogel J (2012) Seven-year trends of CO_2 exchange in a tundra ecosystem affected by long-term permafrost thaw. *Journal of Geophysical Research*, **117**, 1–12.

Trumbore SE, Czimczik CI (2008) An uncertain future for soil carbon. *Science (New York, N.Y.)*, **321**, 1455–6.

Trumbore SE, Harden JW (1997) Accumulation and turnover of carbon in organic and mineral soils of the BOREAS northern study area. *Journal of Geophysical Research*, **102**, 817–28.

Ueyama M, Iwata H, Harazono Y, Euskirchen ES, Oechel WC, Zona D (2013) Growing season and spatial variations of carbon fluxes of Arctic and boreal ecosystems in Alaska (USA). *Ecological Applications*, **23**, 1798–1816.

Vogel J, Schuur EA, Trucco C, Lee H (2009) Response of CO_2 exchange in a tussock tundra ecosystem to permafrost thaw and thermokarst development. *Journal of Geophysical Research*, **114**.

Webb E., Pearman G., Leuning R (1980) Correction of flux measurements for density effects due to heat and water vapour transfer. *Quarterly Journal of the Royal Meteorological Society*, **106**, 85–100.

Welker JM, Fahnestock JT, Jones MH (2000) Annual CO_2 flux in dry and moist arctic tundra: field responses to increases in summer temperatures and winter snow depth. *Climactic Change*, **44**, 139–150.

Welker JM, Fahnestock JT, Henry GHR, O'Dea KW, Chimner R a. (2004) CO_2 exchange in three Canadian High Arctic ecosystems: response to long-term experimental warming. *Global Change Biology*, **10**, 1981–1995.

Winston G., Sundquist E., Stephens B., Trumbore SE (1997) Winter CO_2 fluxes in a boreal forest. *Journal of Geophysical Research*, **102**.

Zimov SA, Davidov SP, Voropaev VY, Prosiannikov S., Semiletov IP, Chapin MC, Chapin FS (1996) Siberian CO2 efflux in winter as a CO2 source and cause of seasonality in atmospheric CO2. *Climactic Change*, **33**, 111–120.

Zuur AF, Ieno EN, Walker NJ, Saveliev AA, Smith GM (2009) *Mixed Effects Models and Extensions in Ecology with R*.

BIOGRAPHICAL SKETCH

Elizabeth E. Webb earned a Bachelor of Arts from Carleton College in 2009 with a major in geology and a concentration in environmental and technology studies. Academically, Elizabeth is interested in anthropogenic impacts on global biogeochemical cycling and local ecosystem function. Her master's research focused on climate change and the alteration of the carbon cycle in northern latitudes. While completing her master's at the University of Florida, Elizabeth also participated in science outreach through PolarTREC (Teachers and Researchers Exploring and Collaborating) and worked with middle school and high school teachers in the field to communicate high latitude science to students in the classroom.